SLAC-PUB-104
May 1965

THE AUTOMATIC PHASING SYSTEM FOR THE STANFORD TWO-MILE LINEAR ELECTRON ACCELERATOR*

C.B. Williams,† A.R. Wilmunder, J. Dobson,‡ H.A. Hogg, M.J. Lee and G.A. Loew
Stanford Linear Accelerator Center
Stanford University, Stanford, California

INTRODUCTION

The automatic phasing system for the Stanford two-mile linear electron accelerator is designed to be capable of adjusting the phases of 240 high power klystrons so that they each contribute maximum energy to the bunched electron beam being accelerated. The two-mile linear accelerator is at present being built by Stanford University, under contract with the U. S. Atomic Energy Commission. A recent aerial view of the site is shown in Fig. 1. The most prominent building is the two-mile long Klystron Gallery which contains the 240 high power klystrons and modulators and all the rf drive and localcontrol equipment together with the electrical, vacuum and water systems. The 10,000 ft. accelerator structure is housed in a reinforced concrete building lying 25 feet below the Klystron Gallery. (See Fig. 2.) It consists of a cylindrical disk-loaded waveguide whose dimensions have been chosen so that it propagates a TM_{01} wave with a phase velocity equal to the velocity of light at 2856 Mc/sec (10.5 cm wavelength). The machine comprises 960 sections, each 10 ft. long, individually supplied with rf power by means of a rectangular waveguide. They are grouped into 30 sectors, each containing 32 sections and a special 10 foot "drift section"

(Paper presented at 1965 G-MTT Symposium, May 5-7, 1965, Clearwater, Florida.)

*Work supported by the U.S. Atomic Energy Commission.
†Presently at the Laboratoire de l'accélérateur linéaire, Orsay, France.
‡Presently at the University of Sheffield, Sheffield, England.

in which the functions of beam steering, focusing, current monitoring and position monitoring are performed. The accelerator is preceded by an injector, which contains an electron gun and special "buncher" sections for initial capture, bunching and acceleration of the electron beam. At the end of the machine there is an elaborate "switchyard" through which the beam may be channelled to various experimental end-stations. Initial operation will be with the machine equipped according to the "Stage 1" design i.e., with one 24 megawatt klystron driving four 10-foot sections, making a total complement of 240 klystrons. The rf drive system and all control systems - including the phasing equipment to be discussed - have been designed so that the number of klystrons may be progressively increased in the future to a maximum of 960. ("Stage 2".) Electron beam currents will be up to 300 milliamps peak, and electron energies will be as high as 20 GeV (Stage 1) and 40 GeV (Stage 2).

After a few feet of acceleration, the electron beam has for all practical purposes attained the velocity of light and is therefore in synchronism with the traveling wave in the disk-loaded waveguide. For maximum energy transfer, the phase of each klystron must be adjusted so that the electron bunches, upon entering the corresponding accelerator sections, ride the crest of the axial electric field wave, E_z. (See Figs. 3 and 4a.) In a perfectly phased accelerator, each electron bunch will maintain this position relative to the rf wave in every section, arriving at the end of the machine with a maximum possible energy

$$V_{Max} = \sum_{n=1}^{N} V_n \qquad (1)$$

where N is the number of accelerator sections and V_n is the maximum energy available from section n. (Fig. 4b.)

If the field is at an incorrect phase, φ_n, when the electron bunch enters section n such that it is displaced from the crest, $E_{z\,max}$, by a phase angle φ_n, the accelerating force acting upon the electron bunch, and consequently the energy gained by it, will be decreased by a factor $\cos \varphi_n$. In general, the total energy gained in the accelerator will be

$$V_{Tot} = \sum_{n=1}^{N} V_n \cos \varphi_n \,. \tag{2}$$

For small values of φ_n we may approximate this to

$$V_{Tot} = \sum_{n=1}^{N} V_n \left(1 - \frac{\varphi_n^2}{2}\right). \tag{3}$$

Assuming that the rf power into each section is the same, this becomes

$$V_{Tot} \simeq VN \left(1 - \frac{\overline{\varphi^2}}{2}\right) \tag{4}$$

where $\overline{\varphi^2}$ is the average value of φ_n^2.

From Eq. (4) it is apparent that if we require the electron energy to be not less than 99.5% of the maximum value, than $\overline{\varphi^2}/2$ must be less than 0.005, or the RMS phasing error must be less than 5 degrees. This phasing tolerance was initially adopted for the two-mile machine.

In addition to the stringent requirement that it shall be capable of adjusting the phase of the rf wave within $\pm$ 5 degrees of the electron beam phase at any point on the accelerator, the ideal phasing system must

function rapidly and reliably, with the minimum interference with accelerator operation.

Early Methods Proposed, and Their Limitations

Several methods for phasing the accelerator were considered in detail before the final choice was made. These will be reviewed very briefly, before proceeding to a detailed discussion of the adopted method.

The first method suggests itself immediately upon examination of Fig. 4b: it is simply to rotate the phase of the rf wave in each section to maximize V_{Tot}. Unfortunately, its lack of sensitivity for a long accelerator with large N is also apparent. If we are to detect a change in phase of ± 5 degrees about the optimum for one klystron in 240 then we must be prepared to measure an energy change of one part 2750. From this it is clear that beam energy maximization is not a very good way of phasing a long machine. The sensitivity can be improved by observing the current in part of the electron beam after dispersion by a spectrometer magnet. The change in current in a certain energy width is observed as the rf phase is rotated. However, this method, which is known as the "current variation detection (CVD) technique"[1] is also insufficiently sensitive, and interferes with the beam available for physics experiments.

Another method is to make direct phase comparisons between the rf feed-lines from adjacent klystrons. However, in order to be sure that the waves in successive accelerator sections are correctly phased within the allowed tolerance, the electrical lengths of all rf lines involved must be known very precisely, not only at the time of installation, but subsequently when the temperature has changed and building movements may have occurred. In any case, such a direct comparison ensures only that all

the rf waves are correctly phased with respect to each other, and not at all with respect to the beam. The latter phase alignment has to be achieved by another method, such as the "CVD" technique mentioned above. (It should be remembered that the CVD technique has a workable sensitivity when it is applied to whole sectors of the machine, instead of to individual klystrons.)

Two further methods of phasing will be touched upon. For a detailed discussion, the reader is referred to the relevant reports.[2-7] These two methods depend upon measurement of changes in resistive and reactive beam loading as the relative phases of beam and rf wave are changed in an accelerator section.

The resistive beam loading method consists of adjusting the phase of each klystron until the rf power remaining at the output of the corresponding section is minimized. Unfortunately, its sensitivity is extremely low, and percentage changes in output power are proportional to the sine of the phase error, so that the sensitivity tends to zero as the phasing approaches the optimum value.

The reactive beam loading method is based on the fact that when the electrons are in the correct position on the rf wave, i.e., "riding the crest" as shown in Fig. 3a, the phase of the output from the accelerator section is the same with the beam on or off. That this is so can be seen from Figs. 4 and 5.

When the electron bunches are correctly phased with respect to the high power accelerating rf wave, the rf wave induced in the accelerator by the electron bunches is such that the fundamental space harmonic of the accelerating and induced waves are 180 degrees out of phase. (Fig. 3b.) Thus the resultant wave, E_t, (Fig. 5a) is in phase with the accelerating

(klystron) wave, E_k . When the bunch "slips" with respect to the klystron wave, a phase shift develops between the klystron and resultant waves, as shown by the vector diagram (Fig. 5b). Thus, by installing a phase bridge between the input and output of the accelerator section, the phase difference between the output wave with the beam off and the output wave with the beam on may be measured and reduced to zero, either manually or automatically.

This method of accelerator phasing is quite feasible, but the sensitivity depends on the beam current and the klystron power, and it does require that the beam be turned on and off, thus interfering with physics experiments.

SELECTED METHOD OF PHASING

Phasing by the "Beam-Induction Technique"

Examination of the latter method of phasing, which involves an indirect measurement of the phase of the beam-induced wave in an accelerator section, leads us to the beam induction method which has been chosen for the two-mile machine.

The principle of the beam induction technique is as follows:

1. With the klystron wave turned off, the phase of the beam-induced wave in the particular accelerator section to be phased is compared with a coherent reference signal of the same frequency.
2. The phase of the reference signal is adjusted to be the same as the beam-induced signal at the place where the comparison is made. (Fig. 6a.)
3. The phase of the reference signal is then locked.
4. The klystron is turned on, and the phase of the klystron wave in the accelerator section is compared with the reference signal.

5. The phase of the klystron signal is adjusted to be 180 degrees away from the phase of the reference signal. (Fig. 6b.)

For the reasons explained above and illustrated in Figs. 4 and 5, the klystron is then optimally phased.

For clarity in the statement of the principle of operations, one over-simplification of the system was made which requires immediate correction: when the phase comparison between beam-induced and reference signals is being made, there is no need to turn the klystron off. Indeed, to do so is very undesirable because removal of rf power from an accelerator section allows it to cool down, with a consequent change in its dimensions and propagation characteristics. Since, for many other reasons, the accelerator is a pulsed machine (rf pulse length approximately 2-1/2 microseconds, pulse repetition frequency 60 to 360 pulses per second), it is only necessary to delay the klystron pulse by a suitable interval, typically 50 microseconds, during the phasing operation, instead of turning it off.

The delayed position of the klystron pulse with respect to the beam pulse is referred to as the "standby" position. Normally, all klystrons being run up to power after repair or replacement will be left operating in the "standby" position, and will be brought to the "accelerate" position (i.e., synchronism with the beam pulse) as additional energy is required for the physics experiment.

Advantages and Problems of the Beam-Induction Technique

There were a number of problems associated with the beam-induction technique which had to be overcome before a workable system was evolved. In this section we shall start by mentioning some of the obvious advantages and then pass to a more detailed discussion of the problems and the

solutions found in each case. As advantages, we can list the following:

1. Of all the methods making use of the beam, it has the best sensitivity, particularly when the beam current becomes very small.
2. The beam and klystron signals are sampled directly at the accelerator, and are transmitted along a common cable to the phase detection circuit in the Klystron Gallery. The phase comparison is therefore essentially direct; the length of the cable does not need to be known, and the attainable sensitivity and accuracy are good.
3. There need be very little interference with physics experiments, because only one klystron at a time need be "set to standby" as the phasing operation progresses along the machine.
4. Klystrons which are placed on "standby" for reasons other than phasing can be maintained correctly phased with respect to the beam, so that they are instantly available for acceleration, on demand.
5. In Stage 1 operation, only eight cables per sector are required to be run from the accelerator housing to an instrumentation and control alcove in the Klystron Gallery.

The first problem to be considered is probably the most serious. It relates to the very large difference between the power levels of the beam-induced and the klystron signals. We have to consider the extremes of the specified operating conditions under which the phasing system will be required to operate, viz., a beam current pulse as low as 1 milliamp, and a klystron peak power input to one 10-foot accelerator section as high as

24 megawatts. The attenuation per 10-foot section is approximately 5 dB, and the beam-induced power is 26 watts per milliamp^2, so that the largest power ratio of the two signals at the end of the 10-foot section is roughly 54 dB.

Well known devices such as the slotted line, "magic T" and hybrid ring are normally used as networks for the phase comparison of two signals. A minimum or a null in the detected output from one arm of these devices indicates a given phase relationship between the two signals. A null is obtained only if the two signals are of equal amplitude. As the difference between the amplitudes of the two signals increases, the phase-indicating null is replaced by a broad minimum, and the balance point becomes increasingly difficult to detect. The method is unreliable when the signals differ by more than 10 dB. Moreover, we require an <u>overall</u> phase detection system which will develop an error signal depending only upon the phase difference between the two input signals. Considering the phase comparison network as just a <u>part</u> of the overall system, we shall show later that its error signal can be permitted to vary by not more than 4 to 1 over the entire range of input signal levels.

Let us consider then the performance of a hybrid ring used as a phase comparison network (Fig. 7). The signals to be compared are applied to arms 1 and 2, arm 3 is terminated in a matched load, and a detector is placed on arm 4. Let the electric field amplitudes of the input signals be E_1 and E_2. Then the output to the detector is given by

$$E_R^2 = \frac{E_1^2}{2} + \frac{E_2^2}{2} - E_1 E_2 \cos\varphi \qquad (5)$$

where φ is the phase difference between E_1 and E_2 at arms 1 and 2.

Let E_2 represent the reference signal and E_1 either the beam-induced or the klystron signal.

If we use a square-law detector, the detector voltage V_D is

$$V_D = k_1 E_R^2 \tag{6}$$

so that

$$\delta V = V_D\Big|_{\varphi+\pi} - V_D\Big|_{\varphi} = k_1 \left[\left(\frac{E_1^2}{2} + \frac{E_2^2}{2} + E_1 E_2 \cos\varphi\right) - \left(\frac{E_1^2}{2} + \frac{E_2^2}{2} - E_1 E_2 \cos\varphi\right)\right] \tag{7}$$

or

$$\delta V = 2k_1 E_1 E_2 \cos\varphi \tag{8}$$

i.e.,

$$\delta V_{max} = 2k_1 E_1 E_2 \quad . \tag{9}$$

Thus, with a square-law detector, the difference in voltage output for a given phase error is proportional to both E_1 and E_2. We have seen that we can expect E_1^2 to vary over a range of 54 dB, so that a square-law detector is very unsatisfactory.

Now, consider a linear detector, for which

$$V_D = k_2 E_R \tag{10}$$

From Eq. (5),

$$E_{R(max)} = \frac{E_1}{\sqrt{2}} \left[1 + \frac{E_2}{E_1}\right] \tag{11}$$

It follows that

$$V_{D(max)} - V_{D(min)} = \delta V_{(max)} = \frac{E_1}{\sqrt{2}} \left[\left(1 + \frac{E_2}{E_1}\right) - \left(1 - \frac{E_2}{E_1}\right)\right]$$

i.e.,

$$\delta V_{max} = \sqrt{2}\ k_2 E_2 \tag{12}$$

This result is much more promising, since the voltage "swing" as the relative phase angle of the two signals as stated depends only on the amplitude of E_2, which can be kept constant.

δV is plotted as a function of the phase difference, φ, in two cases in Fig. 8. These are

a. $E_1 \gg E_2$

b. $E_1 = E_2$

In case a., Eq. (5) becomes

$$E_R^2 \approx \frac{E_1^2}{2}\left[1 - \frac{2E_2}{E_1}\cos\varphi\right] \tag{13}$$

so that

$$V_D \approx k_2 \frac{E_1}{\sqrt{2}}\left[1 - \frac{2E_2}{E_1}\cos\varphi\right]^{\frac{1}{2}}$$

$$\approx k_2 \frac{E_1}{\sqrt{2}}\left[1 - \frac{E_2}{E_1}\cos\varphi\right] \tag{14}$$

Therefore

$$V_D\Big|_{\varphi+\pi} - V_D\Big|_{\varphi} = \delta V = \left[\left(1 + \frac{E_2}{E_1}\cos\varphi\right) - \left(1 - \frac{E_2}{E_1}\cos\varphi\right)\right] \tag{15}$$

i.e.,

$$\delta V = \sqrt{2}\ k_2 E_2 \cos\varphi \tag{16}$$

In case b.,

$$V_D = k_2 E_2 (1 - \cos\varphi)^{\frac{1}{2}} \tag{17}$$

and

$$\delta V = k_2 E_2 \left[(1 + \cos\varphi)^{\frac{1}{2}} - (1 - \cos\varphi)^{\frac{1}{2}}\right]$$

$$= \sqrt{2}\, k_2 E_2 \left(\cos\frac{\varphi}{2} - \sin\frac{\varphi}{2}\right) \tag{18}$$

Both cases give the same δV_{max} .

The sensitivity, $\partial(\delta V)/\partial\varphi$, is $-\sqrt{2}\, k_2 E_2 \sin\varphi$ in case a. , so that as $\delta V \to 0$, the sensitivity is $-\sqrt{2}\, k_2 E_2$.

In case b., $\partial(\delta V)/\partial\varphi$ is

$$\sqrt{2}\, k_2 E_2 \left[-\frac{1}{2}\sin\frac{\varphi}{2} - \frac{1}{2}\cos\frac{\varphi}{2}\right]$$

so that as $\delta V \to 0$, the sensitivity becomes $-k_2 E_2$. In other words, as we permit E_1 to decrease from very large values to equality with E_2 , the sensitivity of null detection decreases only by a factor $\frac{1}{\sqrt{2}}$.

We do not know of the existence of a detector which will remain perfectly linear over the specified range of input powers. The best approximation presently available is a coaxial thermionic diode, which maintains an index of less than 1.2 over the required range. In Appendix I we show that, if the detector has an index of 1.25 over a 50 dB power range, then the detected output voltage will vary by 4 to 1 over that range. It is concluded, then, that the coaxial thermionic diode is adequate. Experiment confirms that this is so.

The detector used is an RCA Type 6173 coaxial thermionic diode mounted in a special housing (Fig. 9). The anode is held in position by spring

fingers and connected to the center conductor of the Type N input rf connector. The detected output is taken from the cathode to a TNC connector on the side of the diode housing. The filament power is supplied via a separate twinaxial connector.

Equation (11) shows that the diode output has a large component, $k_2 E_1 / \sqrt{2}$ and a very small component, $k_2 E_2 / \sqrt{2} \cos\varphi$ which contains the phase error information. We can "cancel out" the unwanted large component by putting a second detector, identical to the first, on arm 3 of the hybrid ring and taking the difference between the two outputs.

The diode resistive loads are connected in opposition by a balancing potentiometer, the wiper of which may be adjusted to offset asymmetries in the hybrid ring, diodes and diode loads, reducing the E_1 component to zero. At the same time the amplitude of the $E_2 \cos\varphi$ component is doubled.

In theory, the differential diode output as described contains the required phase information. If the diodes are balanced, then as the phase angle φ rotates, the differential output will oscillate about zero, passing through zero when $\varphi = (n + \frac{1}{2})\pi$. The direction from which zero is approached with increasing φ may be used to avoid π ambiguity in phase setting. However, such a system, depending on dc balancing, is impracticable to the extent that it presents the second serious problem in the development of the beam-induction phasing system. The long-term stability required of the diodes and the following dc amplifiers would be very difficult to achieve. The problem is avoided by the use of a technique which has become known as "phase wobbling."

The Principle of "Phase Wobbling"

The dc phase-detection system described above is converted to an ac system by phase-modulating the reference signal, E_2 . This artifice immediately removes most of the problems of drift in dc levels, and provides a method of instructing the automatic servo system whether the phase of E_1 is leading or lagging the phase of the reference, E_2 .

Phase wobbling is achieved by the use of a three-port switching circulator in the reference line (see Figs. 10 and 11). The reference signal enters through one port and propagates to the output port either directly or via a third port, depending upon the polarity of the field used to magnetize the ferrite material. The third port is terminated by an adjustable short-circuit, so that the difference between the two path lengths to the output port can be made one half wavelength. The direction of current-flow in the magnetizing coil is reversed before the arrival of each successive beam-induced or klystron rf pulse. Hence the cw reference signal, E_2 , is "square-wave" phase-modulated at 30 c/s so that successive beam-induced or klystron pulses are compared with reference signals which differ in phase by π .

The principle of the phase wobbling technique is essential to the automatic phasing system which has been developed, so that a description of the former introduces the main features of the latter.

A block diagram of the system is shown in Fig. 11. The cw reference signal E_2 is transmitted to the wobbler via a Fox rotary phase-shifter. This type of phase shifter was chosen because the phase shift it introduces is a linear, monotonically increasing function of the angle of rotation of the phase-shifter drum. There are no discontinuities or end-stops.

The wobbler is driven by a 30 c/s square-wave generator, synchronized by a 60 pps trigger. The wobbler output is connected to the hybrid ring, where the accelerator signal E_1 interacts with E_2 as described above. The output ports are terminated by the two thermionic diode detectors, and the differential output is fed into a gated voltmeter.

To understand the operation of the system so far described, we refer to both Fig. 11 and Fig. 12 . Let the Fox phase-shifter be slowly rotated, so that the phase difference φ between E_1 and E_2 at the hybrid ring increases from 0 to 2π in a time $2T_p$, where $2T_p$ is a few seconds. (Fig. 12a and 12b.) The wobbler is phase-modulating E_2 by $\pm \pi/2$ at 30 c/s, so that the phase of E_2 at the hybrid ring changes by π every 1/60 second. Pulses of signal E_1 are arriving from the accelerator at the rate of 60 per second, the pulse length being 1 to 2.5 microseconds. The trigger for the wobbler driver assures that E_2 changes phase in the interval between the arrival of E_1 pulses.

We have seen (Eq. (14)) that the output from a single linear diode is $k_2/\sqrt{2}\,[E_1 - E_2 \cos\varphi]$, so that the balanced differential output from two diodes will be $\sqrt{2}\, k_2 E_2 \cos\varphi$. It follows that, as E_2 is wobbled, the differential diode output pulse amplitudes will change from $\sqrt{2}\, k_2 E_2 \cos\left(\varphi + \frac{\pi}{2}\right)$ to $\sqrt{2}\, k_2 E_2 \cos\left(\varphi - \frac{\pi}{2}\right)$ in a time $T_W = 1/60$ second. (For clarity, the "wobbled" time scale in Fig. 12b has been expanded.)

To see what happens next, the output pulses are further expanded in the top line of Fig. 12c. For reasons which will be discussed later, the pulse amplitudes are sampled by a "gate," 0.2 microseconds wide. The sample is held until the next pulse arrives, so that a 30 c/s square wave is formed, with amplitude proportional to $\cos\left(\varphi + \frac{\pi}{2}\right)$. This wave is

amplified and fed to the control winding of a 2-phase motor which drives the Fox phase-shifter.

Going back to the wobbler driver, part of the square wave output is fed to a 90° delay circuit followed by an amplifier stage, giving a square wave output which is in quadrature with the wobbler drive signal. This energizes the reference winding of the 2-phase motor. Under these conditions the motor will develop a torque proportional to the amplitudes of the applied square waves. The direction of rotation will depend upon whether the control wave leads or lags the reference wave.

From Fig. 12a and b, when $0 < \varphi < \pi$,

$$E_2 \cos\left(\varphi + \frac{\pi}{2}\right) < 0 < E_2 \cos\left(\varphi - \frac{\pi}{2}\right) . \qquad (14)$$

Therefore we connect the motor so that, under these conditions, the phase shifter rotates towards $\varphi = 0$.

It follows that when $\pi < \varphi < 2\pi$,

$$E_2 \cos\left(\varphi + \frac{\pi}{2}\right) > 0 > E_2 \cos\left(\varphi - \frac{\pi}{2}\right) \qquad (15)$$

and the phase shifter rotates towards $\varphi = 2\pi$, which is identical with $\varphi = 0$.

The system always drives away from the unstable null at $\varphi = \pi$ towards the stable null at $\varphi = 0$.

Before proceeding to a description of the complete automatic phasing system, we shall digress briefly to point out further properties of the wobbler technique.

First, it is easy to show that errors which would otherwise be introduced by differing diode characteristics are eliminated by phase wobbling.

This is an important advantage, because it is not possible to obtain a perfectly matched pair over the entire range of signal levels.

Let the output voltages of the two diodes, A and B, on the hybrid ring be

$$V_A = k_A E_A$$

and

$$V_B = k_B E_B \,, \tag{16}$$

where E_A and E_B are the electric field amplitudes of the resultant rf waves in the output arms of the hybrid ring.

Then, with the wobbler in one position,

$$V_A = \frac{k_A}{\sqrt{2}} \left[E_1 + E_2 \cos \left(\varphi + \frac{\pi}{2} \right) \right] \tag{17}$$

and

$$V_B = \frac{k_B}{\sqrt{2}} \left[E_1 - E_2 \cos \left(\varphi + \frac{\pi}{2} \right) \right] \,.$$

With the wobbler reversed,

$$V_A' = \frac{k_A}{\sqrt{2}} \left[E_1 + E_2 \cos \left(\varphi - \frac{\pi}{2} \right) \right]$$

$$= \frac{k_A}{\sqrt{2}} \left[E_1 - E_2 \cos \left(\varphi + \frac{\pi}{2} \right) \right]$$

and similarly,

$$V_B' = \frac{k_B}{\sqrt{2}} \left[E_1 + E_2 \cos \left(\varphi + \frac{\pi}{2} \right) \right] \,. \tag{18}$$

The automatic system indicates a phase balance when the difference between the detected outputs in the two wobbler positions is zero, i.e.,

$$(V_A - V_B) - (V_A' - V_B') = 0 \tag{19}$$

From Eqs. (17) and (18), this condition occurs when

$$\sqrt{2}\, E_2 (k_A + k_B) \cos (\varphi + \frac{\pi}{2}) = 0 . \qquad (20)$$

This will be so when $\varphi = 0 \pm n\pi$, independently of the values of k_A and k_B.

The second point to be made is that imperfections in the switching circulator do not affect phasing accuracy. In Appendix 2 it is shown that if the phase difference introduced by switching from one path to the other is not exactly π, or if the two paths have different insertion losses, no phase error is introduced.

Overall Description of the Automatic Phasing System

We are now in a position to complete the description of the automatic phasing system being installed in the two-mile machine.

A sector has been chosen as the sub-division of the machine for the purpose of phasing. This is a convenient choice since all the necessary status signals concerning the modulators and klystrons are available at the "instrumentation and control" alcove located approximately in the middle of a sector. This reduces the distance for the transmission of control signals necessary in an automatic system. In addition, it means that rf cables are kept short, reducing attenuation and phase drift.

Figure 13 is a schematic of the rf Drive System in one sector. The 476 Mc/s main drive signal is multiplied to 2856 Mc/s, at which point -10 dB of the power is coupled off to provide the reference signal, E_2, for the phasing system. The remainder of the signal is used to drive the sub-booster amplifier, which feeds pairs of pulses (each 2.5 microseconds long and separated by 50 microseconds) at 360 pulse-pairs per second into the sub-drive line of which 60 are used for the phasing system.

The sub-drive line runs the length of one sector. Power is coupled from it at eight points, each coupler feeding one main klystron through an isolator, phase-shifter, attenuator unit. The phase-shifter in this unit is of the type already described. It is coupled to the automatic phasing system, and will be referred to as the "klystron phase-shifter," φ_k . The rf output from each klystron feeds four 10-foot accelerator sections, as shown. The lengths of waveguide runs between the klystron and the four sections are carefully controlled to give the correct phase relation between each section at the design frequency and temperature. No adjustment of the relative phases within each group of four sections is possible after installation. Of course, a change in frequency results in a phase shift between sections, but this is negligible. In addition, it can be shown that the loss of beam energy due to a frequency change is a minimum if the phasing signal is taken from the second or third section of each group of four sections. A 20 dB cross-guide coupler is placed in front of the matched termination at the end of the second or third 10-foot section, and is used to sample the klystron wave and beam-induced wave for phasing purposes.

Figure 14 is a block diagram of the automatic phasing system for an entire sector. The outputs from the third section of each group are transmitted to an eight-position switch which selects one channel at a time and transmits the E_1 signal to the hybrid ring - wobbler - detector system which has been described previously. The switch, wobbler and phase detector are housed in the "RF Detector Panel." The phase-shifter in the reference line to the wobbler is known as the "control phase shifter," φ_c .

The gated voltmeter, servo amplifier, wobbler driver, 90° delay and amplifier are housed in an "electronics panel" together with a "null detector" which determines when the phasing operation is complete by measuring the servo control voltage. The function of the "electronics panel" has also been described in connection with phase-wobbling. The programmer is a special switching unit which ensures that the steps described in the previous section are carried out in sequence, and repeated "down the line" until all eight klystrons in one sector are properly phased.

The operation of the complete system is as follows:

1. When the programmer "start" button is pressed, klystron No. 1 is set to the "standby" pulse position (i.e., delayed 50 microseconds with respect to the beam pulse). Switches in the rf detector panel connect the appropriate accelerator section output to the hybrid ring, and the phase of the beam-induced wave is compared with the reference signal. A typical CRO trace of the video signal at the output of the diode network before phasing is shown in Fig. 15a.
2. The control phase-shifter, φ_c, rotates toward a stable null until the servo amplifier output drops below 2.5 volts. The motor then stops and the null detector indicates that the programmer may advance to the "klystron-phase" position.
3. A brake is applied to φ_c.
4. Provided that klystron No. 1 is operating properly, the "gate" of the gated voltmeter shifts to sample the standby klystron pulse, so that the phase of the klystron wave is compared with the reference.

5. The klystron phase-shifter, φ_k, preceding klystron No. 1 is connected to the electronics panel by the programmer and rotates to a stable null which is made to be π away from the stable null of φ_c by simply reversing two of the leads to the φ_k motor.

   A typical CRO trace of the video signal at the output of the diode network after phasing is shown in Fig. 15b.

6. When the null detector indicates that the phasing error is within the accepted tolerance, the programmer switches to klystron No. 2, setting it to standby and returning No. 1 to accelerate. The phasing cycle is then repeated.

7. The phasing operation continues until all eight klystrons are phased.

8. When the null detector indicates that the last klystron in the sector has been phased, the programmer energizes switches in the rf Detector Panel, connecting a sample signal from the sector sub-drive line to the control phase shifter, φ_c (Fig. 11). At the same time, the other input arm of the hybrid ring gets connected to the output of a "reference cavity" located in the drift section at the end of the previous sector (shown schematically in Fig. 14). This reference cavity is a re-entrant cavity resonant at 2856 Mc/sec whose axis is collinear with the accelerator axis, so that the bunched beam passes through it. Part of the beam-induced output signal from the cavity is used as a normalizing signal for the beam position monitoring system (not part of this system), and part is used to provide a sector phase reference signal.

The phases of the cavity and sub-drive line signals are compared at the hybrid ring, and the automatic servo system rotates the control phase shifter, φ_c , until a stable null is reached with the servo amplifier output voltage below 2.5 volts. At this point, the brake is applied to lock the position of φ_c and the programmer switches itself off. However, the electronics and rf detector panels are not de-energized, so that the phase balance between the cavity and sub-drive line signals continues to be monitored. If a phase drift occurs such that the servo amplifier output voltage exceeds 2.5 volts, a red warning-light appears in the sector instrumentation alcove and in the central control display. The phase drift may be corrected either by automatically re-phasing the sector, or by rotating the phase-shifter preceding the sub-booster (Fig. 13).

DESCRIPTION OF COMPONENTS

Cables for Transmission of Phasing Signals

In order to transmit the rf signals from the section to the rf detector panel with the minimum of loss and yet with some flexibility in installation, a 7/8" coaxial cable is being used. This is a 50 ohm cable with an attenuation constant of 2.8 dB/100 ft. and a peak power handling capacity of over 60 kilowatts. The line will be pressurized with dry air at 5 lbs/square inch above atmospheric pressure and sealed off.

The variation in phase shift through the cable due to ionizing radiation has been calculated and has been shown to be negligible for the radiation levels anticipated in the accelerator housing and for the lengths of cable which will be exposed.

The RF Detector Panel

The wobbler and phase detection components of the rf detector panel have already been described. The 8-position selector switch is actually made up as a tree of coaxial switches. Eight SPST switches feed two SP4T switches which are linked by one SP2T switch. This chain has the advantages that it can be constructed from readily available commercial switches, and gives an inter-channel cross-talk isolation of about 100 dB, which is in excess of this system's requirements.

In the rf detector panel, provision is also made for manually switching to any klystron, and for monitoring rf and video signals.

The Phase-Shifter Units

The characteristics of the klystron and control phase shifters, φ_k and φ_c, have already been discussed. Each phase-shifter drum has an electromagnetic brake which is applied when the 2-phase motor is de-energized. In addition, the klystron phase-shifters have isolators and two attenuators built into an integral unit (Fig. 15). One attenuator is manually controlled and is used to set the klystron drive level; the other is controlled by a dc motor and is automatically inserted if a fault appears in the klystron. There is a dual directional coupler on the output, for monitoring the power transmitted to and reflected from the klystron.

The Electronics Unit

The Square-Wave Generator

The square-wave generator actually consists of a divide-by-two circuit and a reference amplifier which provide a master time and phase supply for the automatic phasing system. A trigger pulse, selected by the programmer, is used to trigger a divide-by-two multivibrator. The output of this

multivibrator drives an amplifier to provide power to operate the phase wobbler and the 90° delay and servo reference amplifier. These units are of the printed circuit type of construction, as are all other electronic devices described in this section.

The 90° Delay and Amplifier

These units provide a quadrature reference voltage to operate the two-phase servo motors used to drive the klystron and control phase shifter. The unit consists of two monostable multivibrators and an amplifier identical to the reference amplifier. The first multivibrator is triggered by a signal from the master "divide-by-two" and acts as a quarter cycle time delay. At the end of one quarter cycle, the circuit emits a pulse to trigger the second multivibrator. The second multivibrator drives the servo amplifier, the output of which is essentially a 30 cps square wave delayed by one quarter of a cycle from the master square wave.

The Gated Voltmeter

If the accelerator is operating at the incorrect frequency of if the section is at the wrong temperature, a phase change will occur across the transient part of the beam induced pulse. In order to minimize any phasing errors which could occur as a consequence of this transient, it is necessary that the phase comparison be made only in the steady state condition. For this reason a gated voltmeter has been developed which samples only a 0.2 microsecond portion of the pulse. The gated voltmeter is basically a sample and hold circuit with a 0.2 microsecond sample time. The position of the sample gate is determined by a trigger selected by the programmer. Once a signal is sampled, the voltmeter retains the information, subject to a decay determined by the 10 second time constant of the hold circuit.

A gain of ten is provided by a pre-amplifier within the voltmeter to amplify low level signals. The time constant of the sample circuit is 40 nanoseconds, so that signals of different levels can be sampled each gate time and the hold circuit will be charged to over 90% of the level of each sample.

The servo control amplifier is driven from the output of the gated voltmeter and amplifies this signal to the level necessary to drive the control winding of the servo motor.

The Null Detector

The null detector is used to determine the end of each phasing operation. As the phase shifters rotate to bring the system to an in-phase condition, the signal from the servo control amplifier decreases in amplitude. This decrease in amplitude is detected by a diode bridge. When a null is reached, a relay in the programmer is released, allowing the programmer to advance to the next step.

The Programmer

The programmer is basically a switching system which selects the klystrons in numerical order, within a sector, and steps through a sequence of events with the final objective of adjusting the phase of each klystron correctly with respect to the electron beam in the accelerator.

The programming is accomplished by a single stepping switch and a subprogram, consisting of two relays. Three auxiliary relays are used to determine the klystron status and the end of each step. A stepping generator provides pulses to operate the stepping switch used for the klystron selector. A completed programmer is shown in Fig. 19. Despite its complex function, the unit occupies only 3-1/2 inches of rack space.

Experimental Results Obtained So Far

The automatic phasing system has been operating in the first two sectors of the machine since early February. These two sectors, comprising 660 feet of the 2-mile accelerator, are being used to evaluate the basic design of the accelerator and ancillary equipment while the rest of the machine is being built.

Initially, some trouble was experienced with the thermionic diode detectors. Attenuators in the rf detector panel were set such that the level of accelerator signal powers was too high. Under these conditions, the diode plate voltage exceeded the specified maximum value when the klystron signals were being detected. This caused rapid drift of the diode balance point, which could not be accepted by the gated voltmeter. We found that it was possible to reduce the rf power level such that the power per diode from a 1 milliamp accelerator beam was as low as 1 milliwatt. At this power level, the departure of the diode level from linearity was not sufficient to cause the gated voltmeter input to exceed the 4 to 1 voltage ratio limit.

Since these adjustments have been made, the automatic system has worked very satisfactorily. The average time taken to phase a sector which is initially random-phased is about one minute. A sector which has been previously phased can be "trimmed" in 43 seconds.

Recently tests were performed to determine the resetting accuracy of this Automatic Phasing System. All phase shifters were marked after being automatically set. The entire sector was randomly phased manually and then automatically rephased. The worst error measured was 3°, with most phase shifters returning to within 1° of their previous positions.

In addition to performing the essential function for which it was designed, the phasing system is beginning to be recognized as a very useful diagnostic tool. For instance, if the beam-induced pulse is observed as phasing proceeds down a sector, sudden decreases in the pulse amplitudes between adjacent test points immediately indicate loss of beam due to local mis-steering. Sub-drive line and klystron phase jitter, and a variety of other mal-functions in the drive system can be easily recognized.

ACKNOWLEDGEMENT

The authors are indebted to Dr. R. B. Neal and Mr. D. J. Goerz for their initial contributions in formulating the idea of beam-induction phasing, and to Messrs. G. Jackson, Jr., J. R. Bordenave, P. V. Lee and K. E. Holladay for their assistance in developing and testing the prototype system.

APPENDIX I

It was shown in the text that, if two signals E_1 and E_2 were fed into arms 1 and 2 of a hybrid ring, the output voltage from a detector placed on arm 4 (with arm 3 matched) would be proportional only to the phase difference between E_1 and E_2, and the amplitude of E_2, if the detector were linear and $E_1 \gg E_2$.

In this appendix we consider the effect of increasing the index of detection to values greater than unity.

As before, the resultant signal at the detector is

$$E_R^2 = \frac{E_1^2}{2} + \frac{E_2^2}{2} - E_1 E_2 \cos \varphi \qquad (5)$$

so that

$$E_{R(max)} = \frac{E_1}{\sqrt{2}} \left[1 + \frac{E_2}{E_1} \right] \qquad (21)$$

and

$$E_{R(min)} = \frac{E_1}{\sqrt{2}} \left[1 - \frac{E_2}{E_1} \right] \qquad (22)$$

Let the detector have an index n, so that

$$V_D = k E_R^n \quad . \qquad (23)$$

Then

$$V_{D(max)} = k' E_1^n \left[1 + \frac{E_2}{E_1} \right]^n \qquad (24)$$

and

$$V_{D(min)} = k' E_1^n \left[1 - \frac{E_2}{E_1}\right]^n \tag{25}$$

where

$$k' = \frac{k}{2^{n/2}} \quad . \tag{26}$$

Again assuming $E_1 \gg E_2$, we can expand equations (24) and (25), giving

$$V_{D(max)} = k' E_1^n \left[1 + n \frac{E_2}{E_1} + \frac{n(n-1)}{2!} \frac{E_2^2}{E_1^2} + \cdots\right] \tag{27}$$

and

$$V_{D(min)} = k' E_1^n \left[1 - n \frac{E_2}{E_1} + \frac{n(n-1)}{2!} \frac{E_2^2}{E_1^2} - \cdots\right] \tag{28}$$

Letting

$$V_{D(max)} - V_{D(min)} = \delta V_{max} \tag{29}$$

we have

$$\delta V_{max} = 2 k' E_1^n \left[n \frac{E_2}{E_1} + \frac{n(n-1)(n-2)}{3!} \frac{E_2^3}{E_1^3} + \cdots\right] \tag{30}$$

The series converges rapidly for $E_1 \gg E_2$ and $1 < n < 2$, so that the above two terms are sufficient for practical purposes. Let E_1 vary between a lower limit E_b and an upper limit E_a, and let the values of δV_{max} at these limits be $\delta V_b(max)$ and $\delta V_a(max)$ respectively.

Then

$$\frac{\delta V_a(\max)}{\delta V_b(\max)} = R = \frac{E_a^n}{E_b^n} \cdot \frac{\left[n \frac{E_2}{E_a} + \frac{n(n-1)(n-2)}{3!} \frac{E_2^3}{E_a^3} \right]}{\left[n \frac{E_2}{E_b} + \frac{n(n-1)(n-2)}{3!} \frac{E_2^3}{E_b^3} \right]} \tag{31}$$

or

$$R = \frac{E_a^{n-1}}{E_b^{n-1}} \frac{\left[1 + \frac{(n-1)(n-2)}{3!} \cdot \frac{E_2^2}{E_a^2} \right]}{\left[1 + \frac{(n-1)(n-2)}{3!} \cdot \frac{E_2^2}{E_b^2} \right]} \tag{32}$$

We assume that $E_1 \gg E_2$ even at its lower limit, E_b, so that the right hand terms are vanishingly small, and Eq. (32) reduces to

$$R = \frac{E_a^{n-1}}{E_b^{n-1}} \quad . \tag{33}$$

As the phase angle between E_1 and E_2 rotates, R is the ratio of the detector voltage "swing" at the extremes of the given range of E_1 amplitudes, for a detection index n.

Equation (33) may be written

$$\frac{20}{(n-1)} \log R = 20 \log \frac{E_a}{E_b} \quad . \tag{34}$$

This expression is plotted in Fig. 16. The right hand side of Eq. (34) gives the power range in dB for signal E_1.

It can be seen from Fig. 16 that if an output voltage variation, R, of 4 to 1 is permitted for a 50 dB range of signal levels, the detector can have an index of detection as high as 1.25.

APPENDIX II

This appendix examines the effect of using a wobbler in which the lengths of the two paths do not differ by exactly one half a wavelength, and the insertion losses of the two paths are not exactly equal.

Referring to Fig. 18 and Eq. (5),

$$V_A = \frac{k_2}{\sqrt{2}} \left[E_1^2 + E_2^2 + 2E_1 E_2 \cos\left(\varphi - \frac{\pi}{2}\right) \right]^{\frac{1}{2}} \tag{35}$$

and

$$V_B = \frac{k_2}{\sqrt{2}} \left[E_1^2 + E_2^2 - 2E_1 E_2 \cos\left(\varphi - \frac{\pi}{2}\right) \right]^{\frac{1}{2}} \tag{36}$$

for the first wobbler path, using linear diodes.

Similarly,

$$\begin{aligned} V_A' &= \frac{k_2}{\sqrt{2}} \left[E_1^2 + (AE_2)^2 + 2AE_1 E_2 \cos\left(\varphi + \frac{\pi}{2} + \Delta\right) \right]^{\frac{1}{2}} \\ &= \frac{k_2}{\sqrt{2}} \left[E_1^2 + (AE_2)^2 - 2AE_1 E_2 \cos\left(\varphi - \frac{\pi}{2} + \Delta\right) \right]^{\frac{1}{2}} \end{aligned} \tag{37}$$

and

$$V_B' = \frac{k_2}{\sqrt{2}} \left[E_1^2 + (AE_2)^2 + 2AE_1 E_2 \cos\left(\varphi - \frac{\pi}{2} + \Delta\right) \right]^{\frac{1}{2}} \tag{38}$$

for the second wobbler path.

If we assume that Δ is small, and that phase balance will occur around $\varphi = 0$ (see text), then the above equations may be reduced to

$$V_A = \frac{k_2}{\sqrt{2}} \left[(E_1^2 + E_2^2)^{\frac{1}{2}} + \frac{E_1 E_2 \cos(\varphi - \frac{\pi}{2})}{(E_1^2 + E_2^2)^{\frac{1}{2}}} \right] \tag{39}$$

$$V_B = \frac{k_2}{\sqrt{2}} \left[(E_1^2 + E_2^2)^{\frac{1}{2}} - \frac{E_1 E_2 \cos(\varphi - \frac{\pi}{2})}{(E_1^2 + E_2^2)^{\frac{1}{2}}} \right] \tag{40}$$

$$V_A' = \frac{k_2}{\sqrt{2}} \left[\left\{ E_1^2 + (AE_2)^2 \right\}^{\frac{1}{2}} - \frac{AE_1 E_2 \cos(\varphi - \frac{\pi}{2} + \Delta)}{\left\{ E_1^2 + (AE_2)^2 \right\}^{\frac{1}{2}}} \right] \tag{41}$$

$$V_B' = \frac{k_2}{\sqrt{2}} \left[\left\{ E_1^2 + (AE_2)^2 \right\}^{\frac{1}{2}} + \frac{AE_1 E_2 \cos(\varphi - \frac{\pi}{2} + \Delta)}{\left\{ E_1^2 + (AE_2)^2 \right\}^{\frac{1}{2}}} \right] \tag{42}$$

Phase balance is indicated when the difference between the detected output in the two wobbler positions is zero, i.e.,

$$(V_A - V_B) - (V_A' - V_B') = 0 \tag{43}$$

which is Eq. 19 in the text.

Substituting, we find that

$$\frac{\cos(\varphi - \frac{\pi}{2})}{(E_1^2 + E_2^2)^{\frac{1}{2}}} = \frac{-A \cos(\varphi - \frac{\pi}{2} + \Delta)}{\left\{ E_1^2 + (AE_2)^2 \right\}^{\frac{1}{2}}} \tag{44}$$

By expanding $\cos(\varphi - \frac{\pi}{2} + \Delta)$, Eq. (44) may be written as

$$\tan(\varphi - \frac{\pi}{2}) = \cot \Delta + \frac{\left\{ E_1^2 + (AE_2)^2 \right\}^{\frac{1}{2}}}{A(E_1^2 + E_2^2)^{\frac{1}{2}}} \cdot \frac{1}{\sin \Delta} \tag{45}$$

It can be seen from Eq. (45) that when $\Delta = 0$ (i.e., the phase difference between the two paths is exactly π) then $\varphi - \frac{\pi}{2} = (2n + 1)\frac{\pi}{2}$, and

$\varphi = 0 + n\pi$ for all values of E_1, E_2 and A. Consequently no phase error arises.

If A = 1, so that the insertion loss is the same for the two paths, then

$$\tan\left(\varphi - \frac{\pi}{2}\right) = \cot \Delta + \frac{1}{\sin \Delta}$$

This is independent of E_1 and E_2. Therefore, although a shift in the position of the null occurs, it is not a function of the signal level so that no phase error is introduced.

REFERENCES

1. R. Belbéoch and C. B. Williams, "Current variation detection technique of phasing linear electron accelerators," Internal Memorandum, Stanford Linear Accelerator Center, Stanford University, Stanford, California, November 1962.
2. W. J. Gallagher et al. (Drive and Phasing Committee), "Methods for phasing long linear accelerators," Report No. M-101, Stanford Linear Accelerator Center, Stanford University, Stanford, California, November, 1958.
3. W. J. Gallagher et al. (Drive and Phasing Committee), "Methods of driving long linear accelerators," Report No. M-102, Stanford Linear Accelerator Center, Stanford University, Stanford, California, December, 1958.
4. D. J. Goerz and R. B. Neal, "Phasing a linear accelerator from rf phase shift due to beam loading interaction," Report No. M-103, Stanford Linear Accelerator Center, Stanford University, Stanford, California, December, 1958.
5. R. B. Neal et al. (Drive and Phasing Committee), "Comparison of methods of phasing long linear accelerators," Report No. M-104, Stanford Linear Accelerator Center, Stanford University, Stanford, California, December, 1958.
6. R. B. Neal, "Transient beam loading in linear electron accelerators," Report No. ML-388, Microwave Laboratory, Stanford University, Stanford, California.
7. G. A. Loew, "Non-synchronous beam loading in linear electron accelerators," Report No. ML-740, Microwave Laboratory, Stanford University, Stanford, California.

FIGURE CAPTIONS

1. Overall view of the accelerator, showing two-mile long service building.
2. Accelerator cross section; looking east in direction of beam.
3. RF field and electron bunch distribution in accelerator structure.
4. Illustrating the effect of imperfect phasing.
5. Vector diagram illustrating principle of phasing accelerator section by reactive beam loading method.
6. Illustrating beam-induction method of phasing accelerator.
7. Hybrid ring phase comparator.
8. δV vs ϕ for linear diodes.
9. Thermionic diode and housing.
10. Switching circulator used as phase wobbler.
11. Block diagram of phase-wobbling system.
12. Illustrating the application of phase wobbling to an automatic phasing system.
13. Drive system schematic for one section of the machine, showing how the signals for the phasing system are derived.
14. Block diagram of automatic phasing system for one sector.
15. Typical CRO trace of the video signal at the output of the diode network.
16. An isolator, phase shifter, attenuator unit.
17. Illustrating the effect of increasing the diode index of detection.
18. Illustrating the effect of an imperfect wobbler.
19. Phasing programmer.

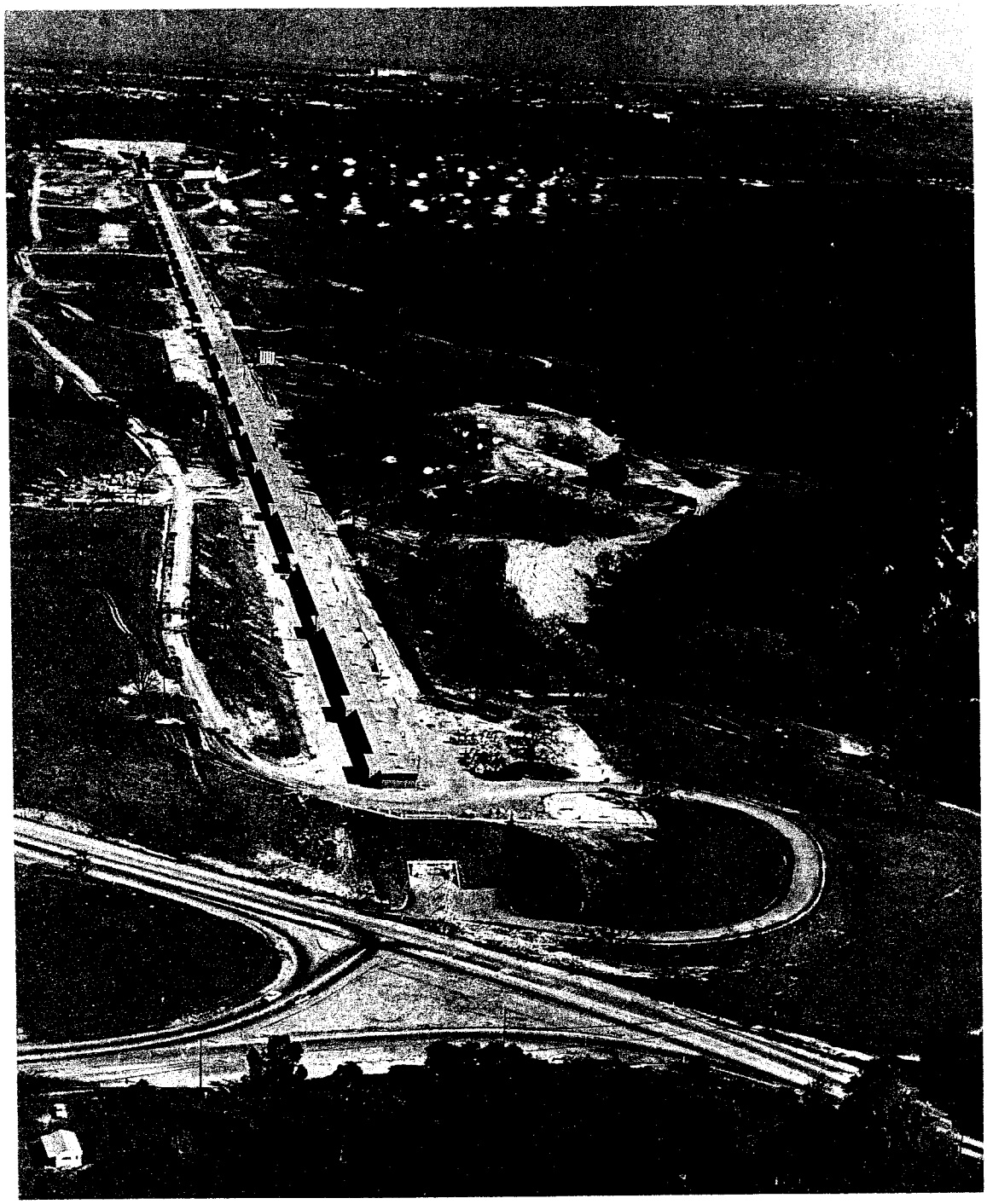

Fig. 1

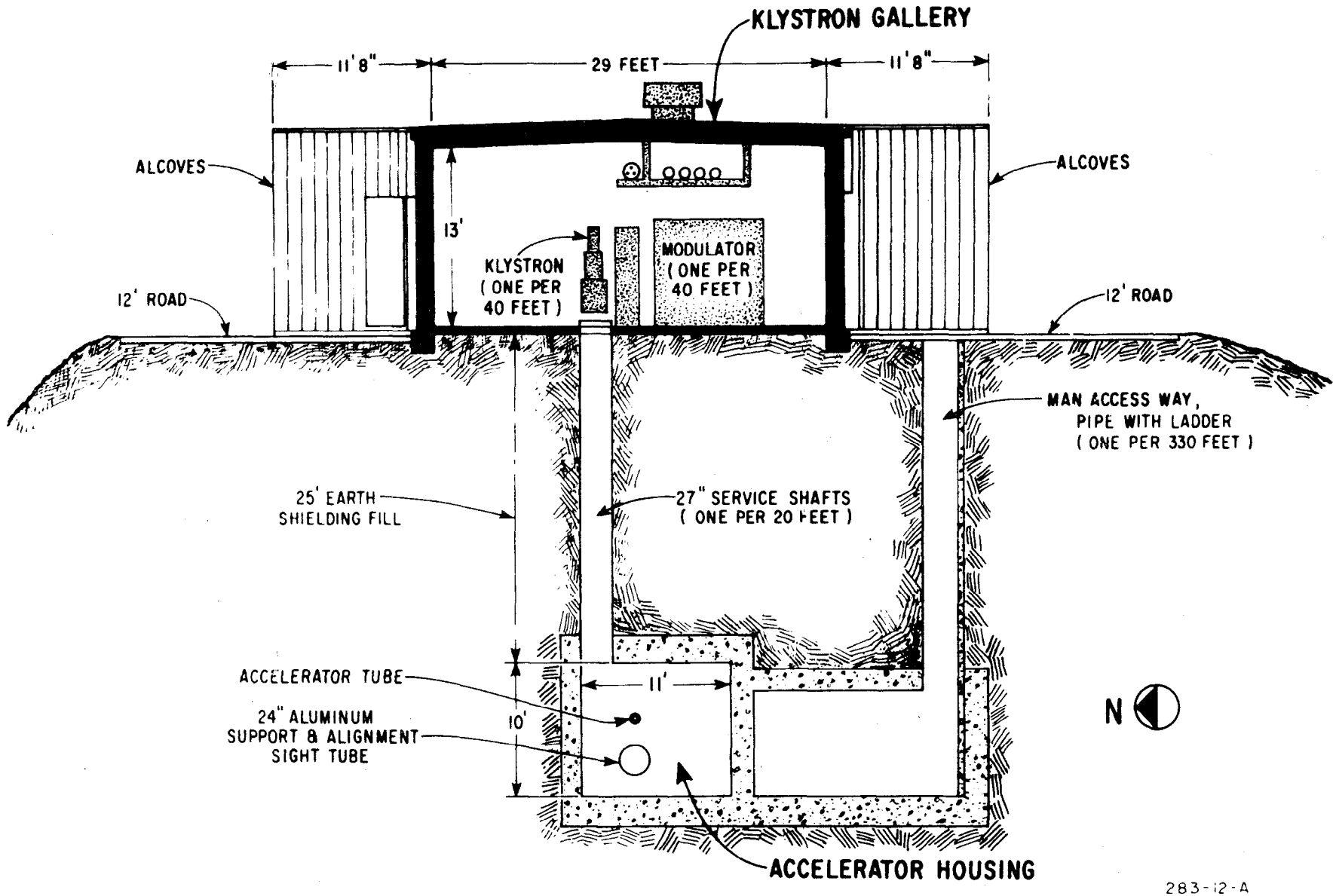

ACCELERATOR CROSS SECTION

LOOKING EAST IN DIRECTION OF BEAM

Fig. 2

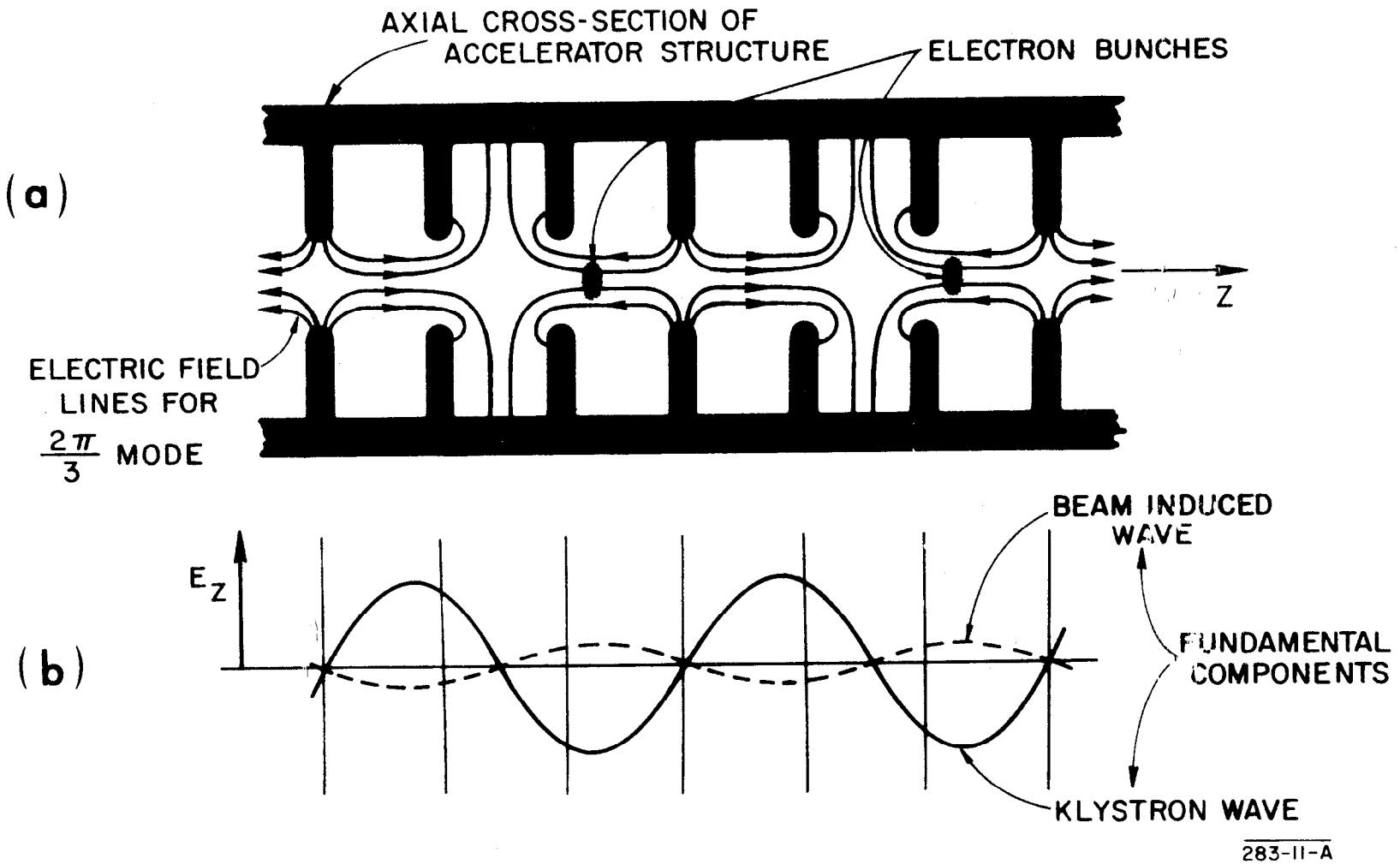

FIG.3--RF FIELD AND ELECTRON BUNCH DISTRIBUTION IN ACCELERATOR STRUCTURE.

ϕ IS THE PHASE ANGLE OF THE CENTRAL ELECTRON WITH RESPECT TO THE WAVECREST.

a)

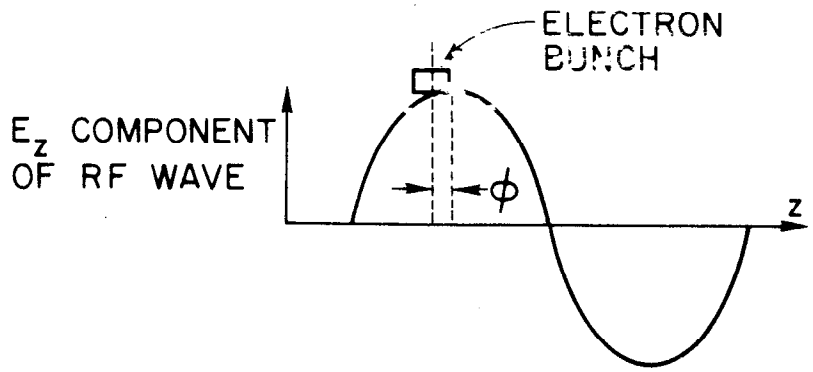

b)

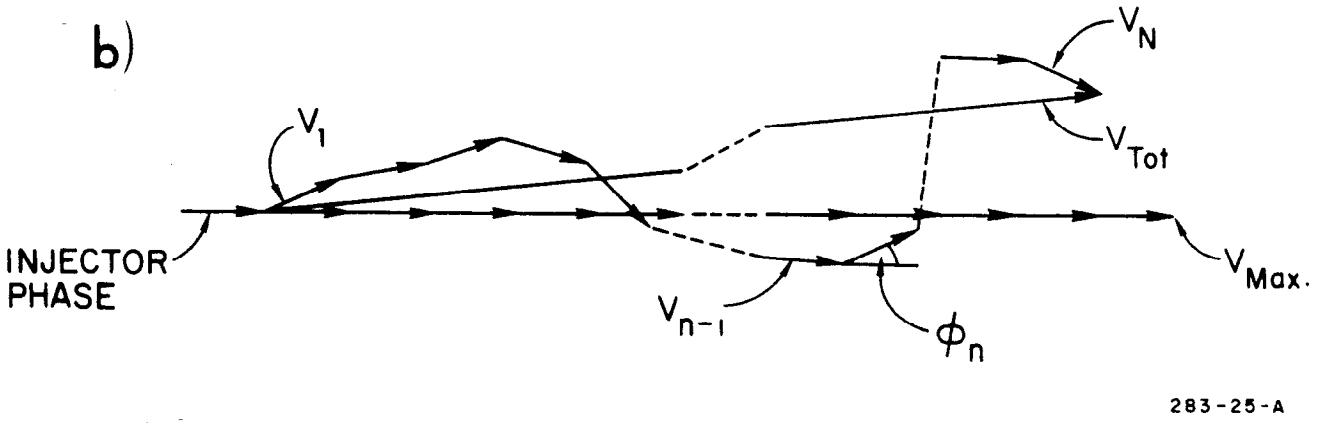

FIG. 4 - ILLUSTRATING THE EFFECT OF IMPERFECT PHASING.

(a) ORIENTATION OF FIELD VECTORS WHEN PHASING IS CORRECT

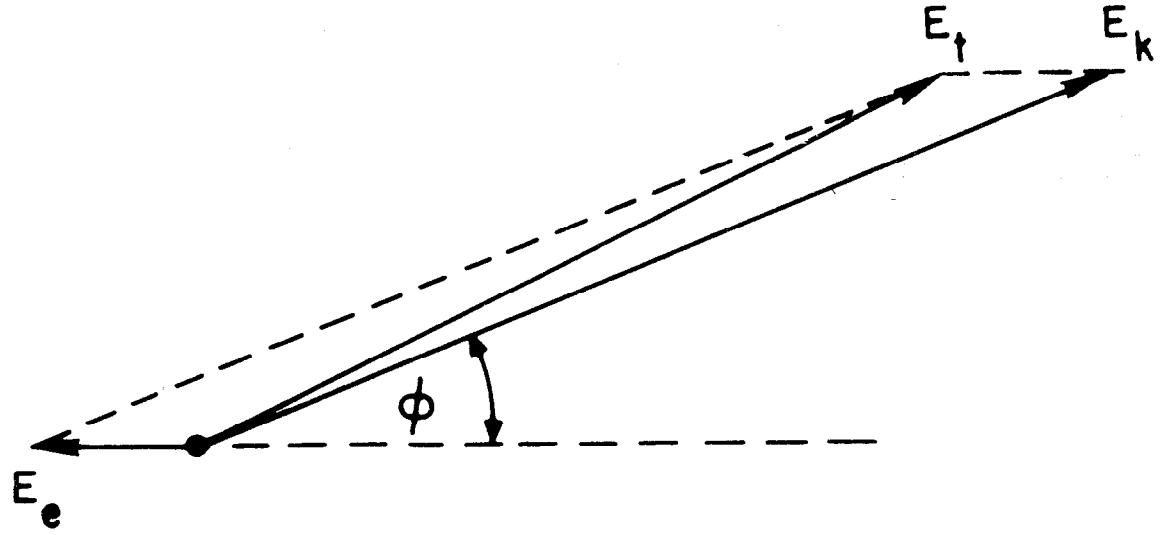

(b) ORIENTATION OF FIELD VECTORS WHEN PHASING IS INCORRECT

283-3-A

FIG. 5 -- VECTOR DIAGRAM ILLUSTRATING PRINCIPLE OF PHASING ACCELERATOR SECTION BY REACTIVE BEAM LOADING METHOD.

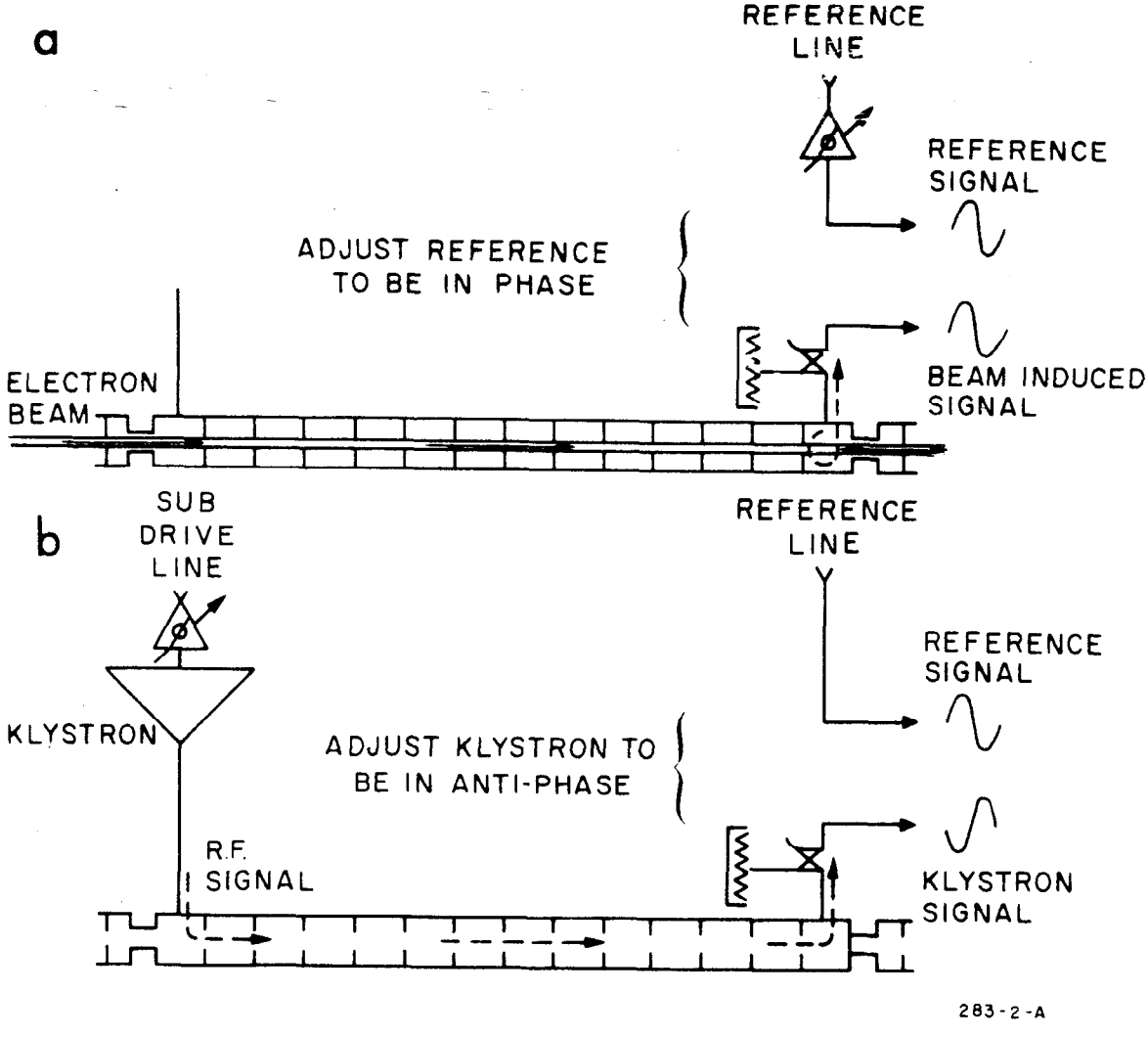

Fig.6--ILLUSTRATING BEAM-INDUCTION METHOD OF PHASING ACCELERATOR

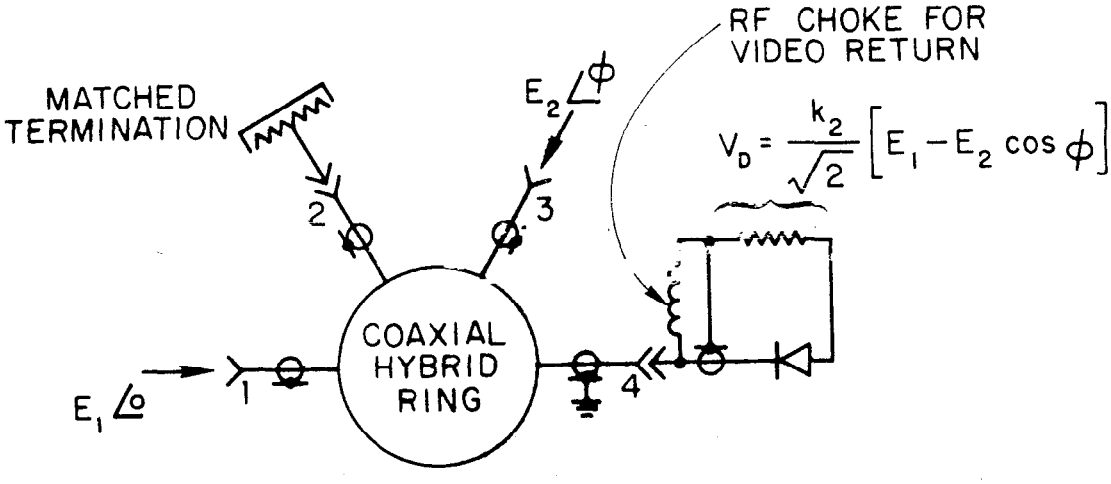

(a)

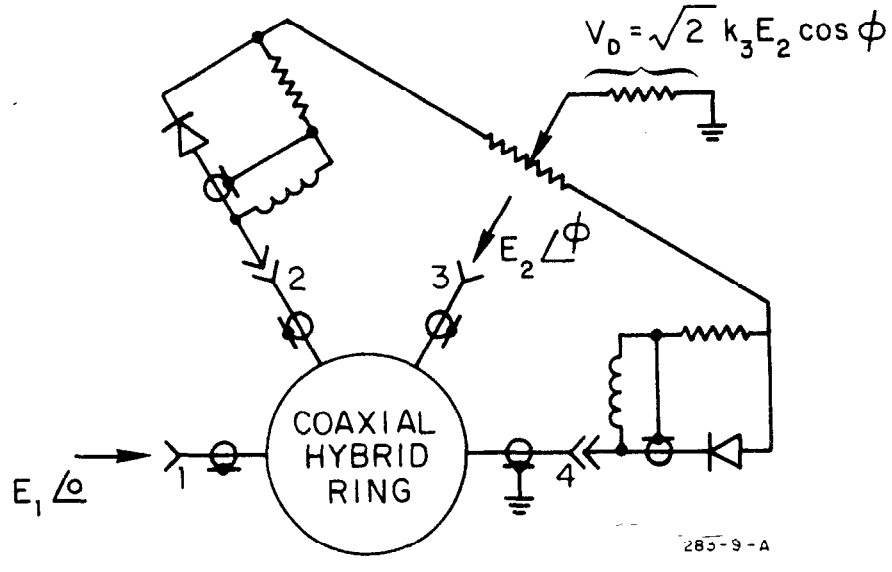

(b)

FIG. 7 - HYBRID RING PHASE COMPARATOR.

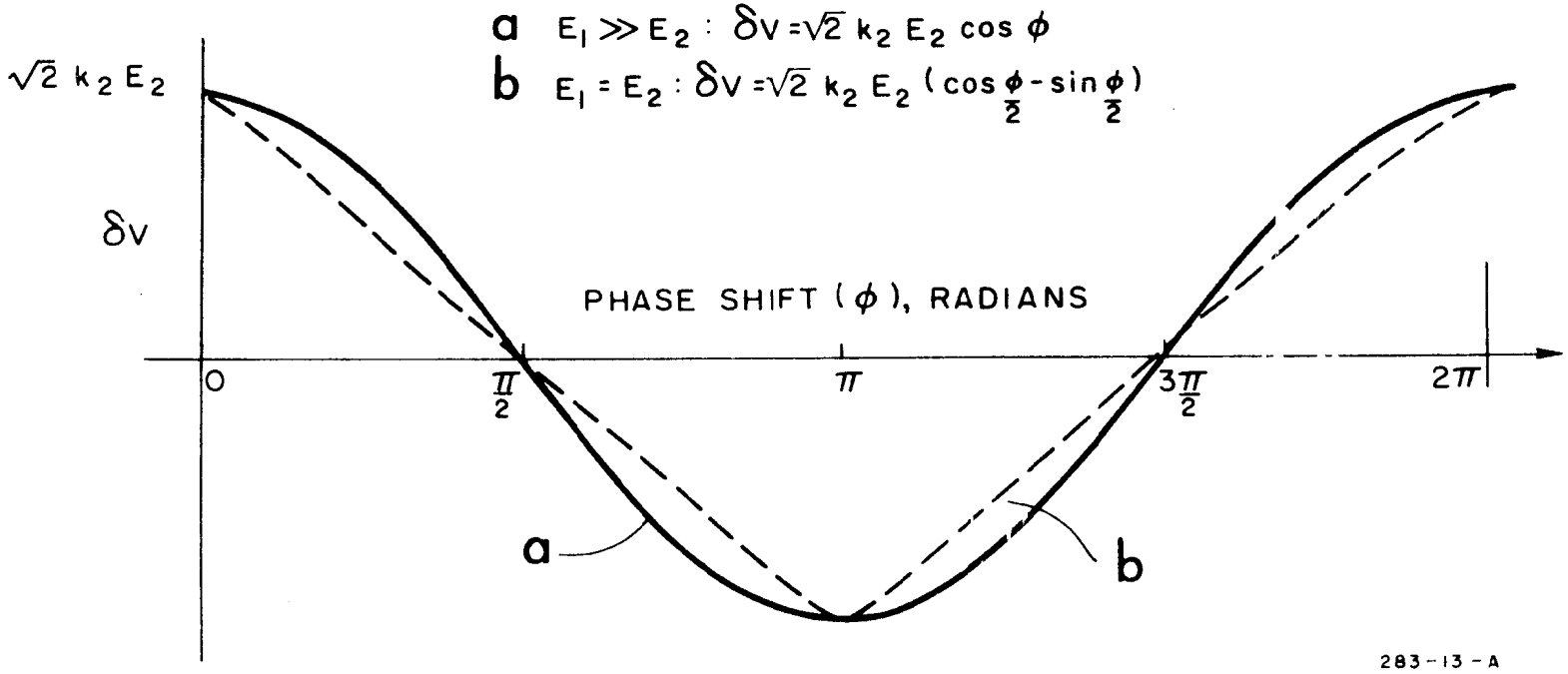

Fig 8--δV vs ϕ FOR LINEAR DIODES

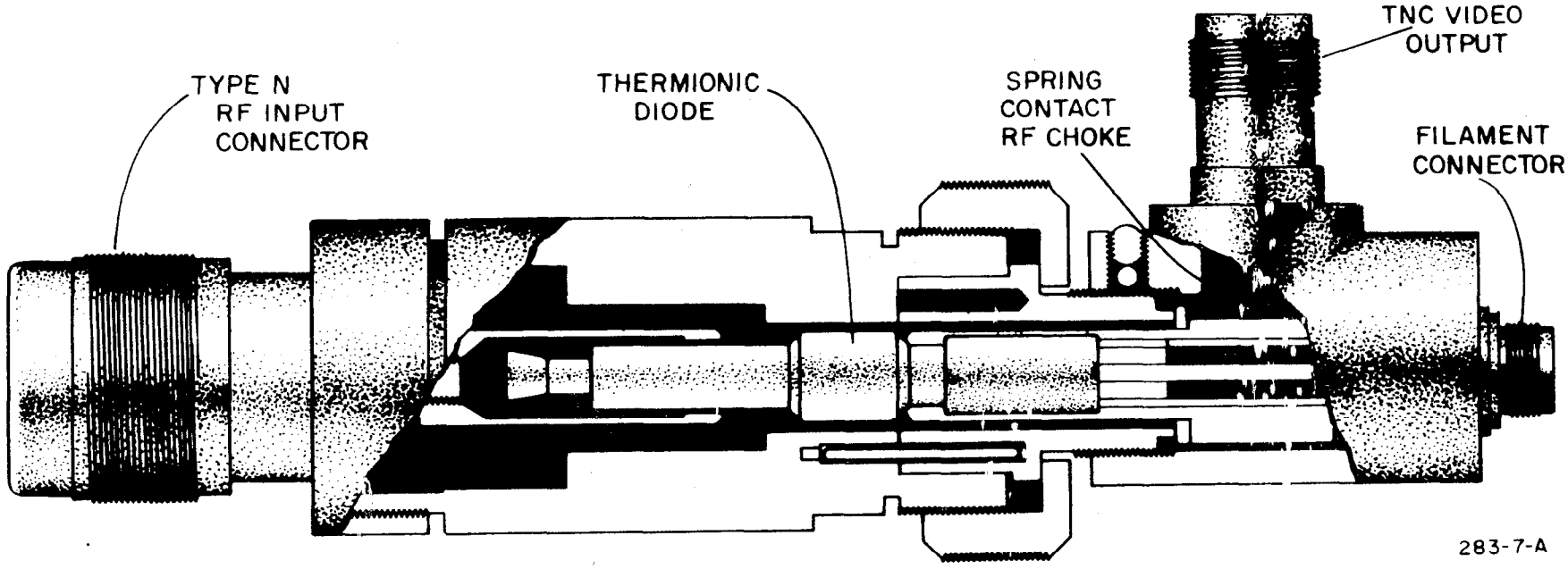

FIG. 9 -- THERMIONIC DIODE AND HOUSING

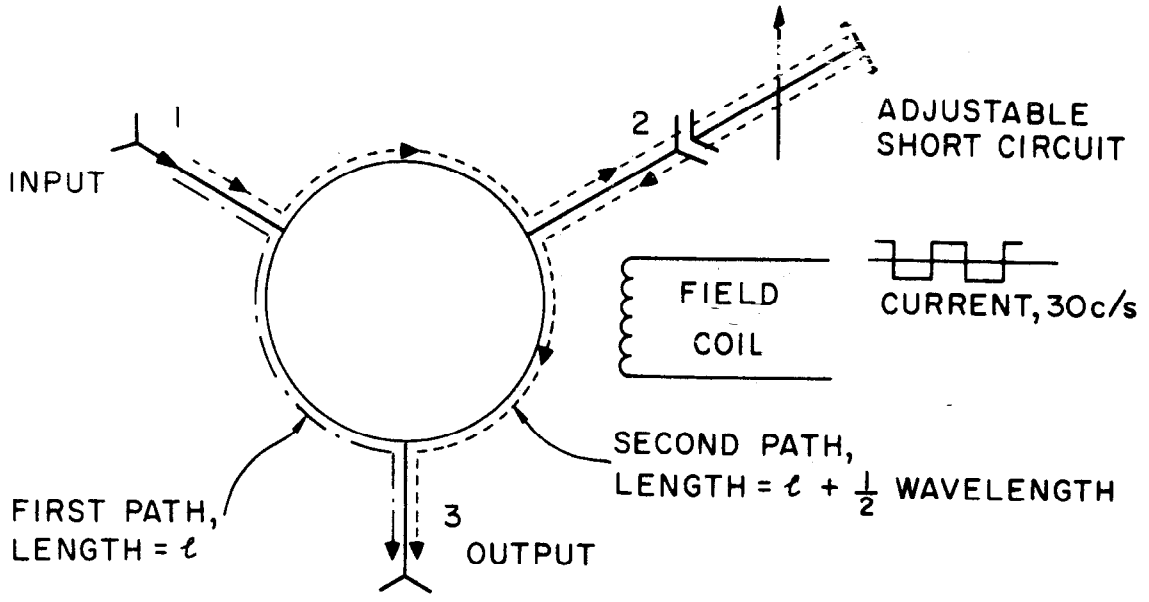

Fig. 10--SWITCHING CIRCULATOR USED AS PHASE WOBBLER

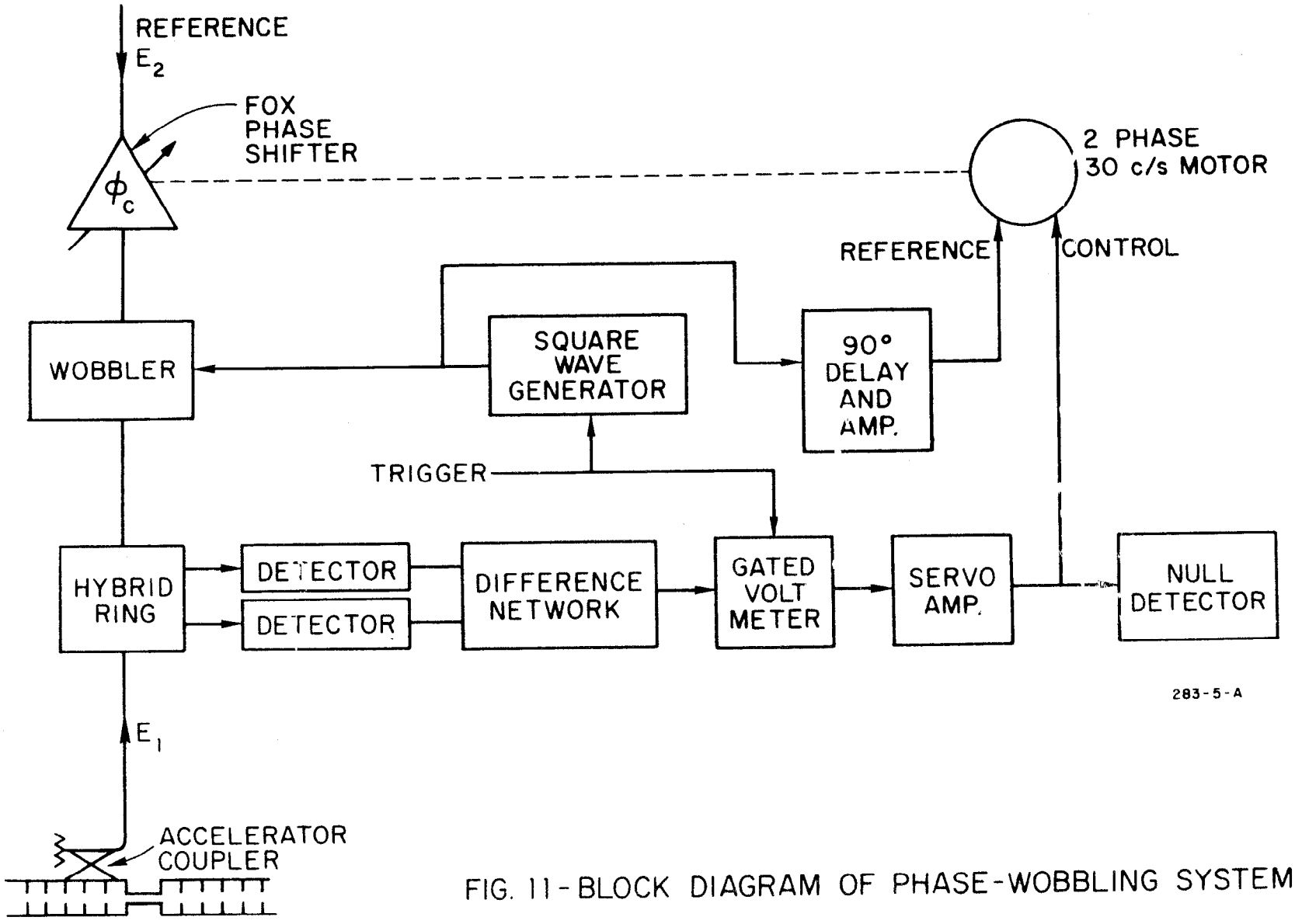

FIG. 11 - BLOCK DIAGRAM OF PHASE-WOBBLING SYSTEM.

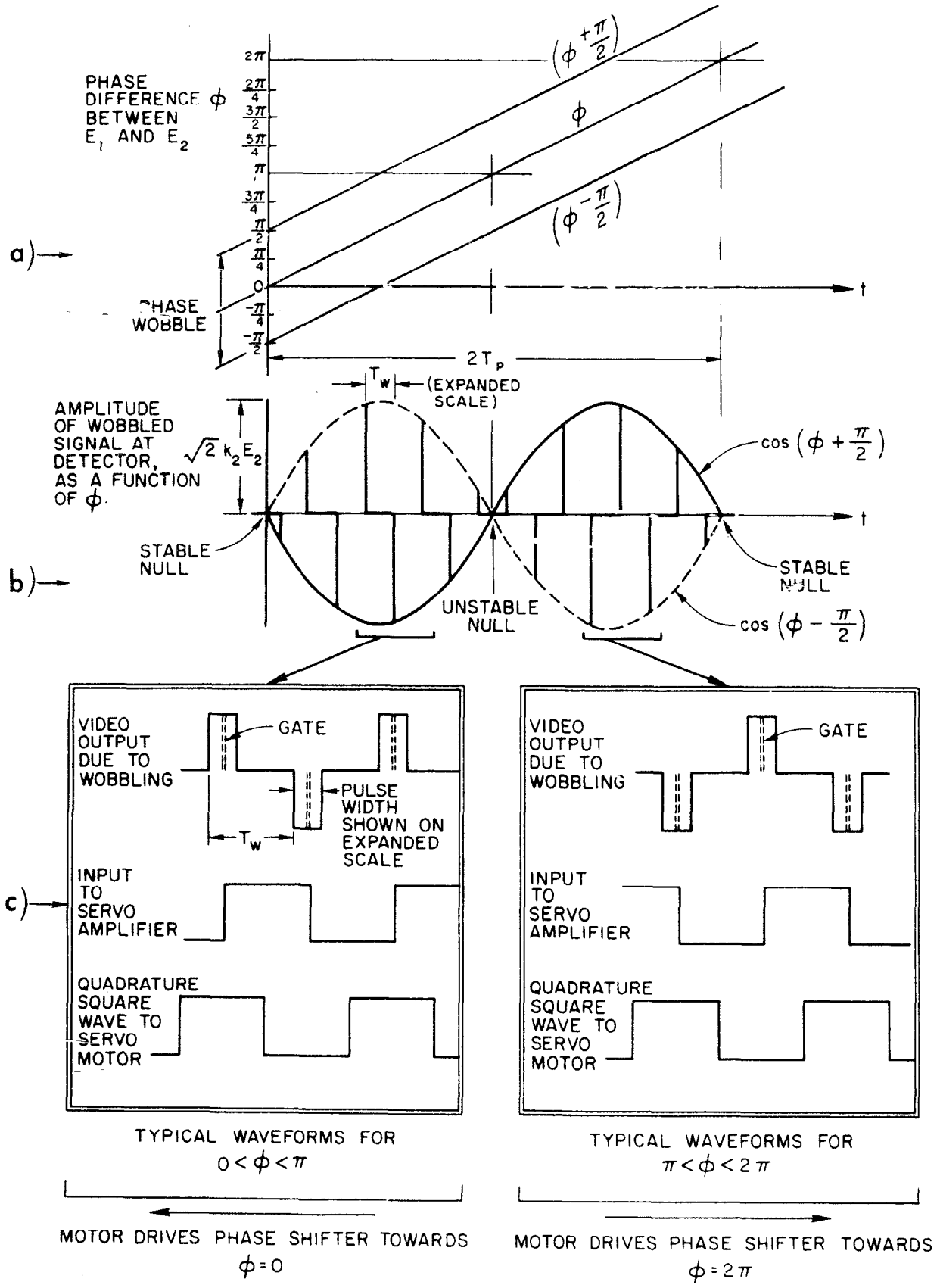

FIG. 12 - ILLUSTRATING THE APPLICATION OF PHASE WOBBLING TO AN AUTOMATIC PHASING SYSTEM.

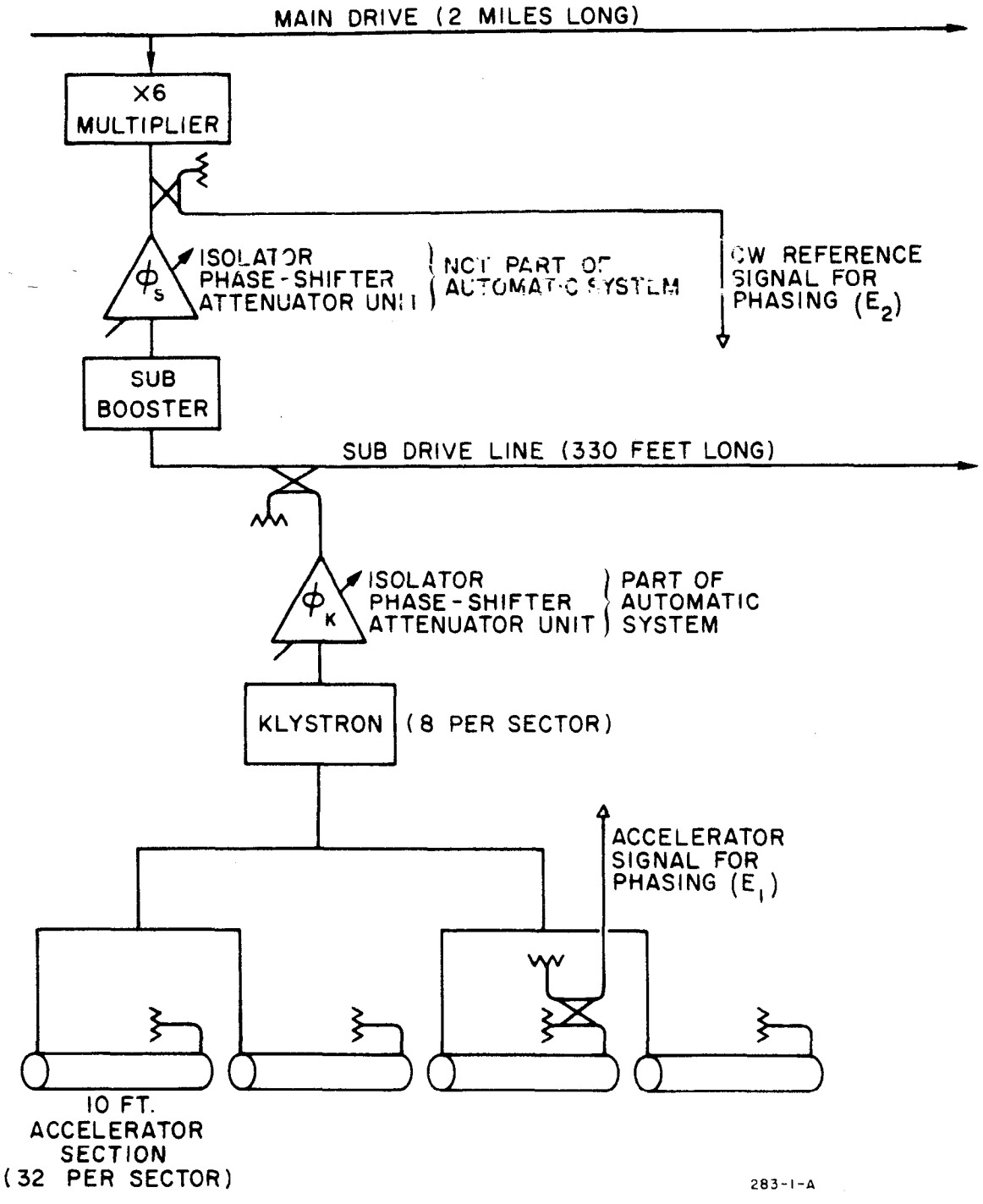

FIG. 13 - DRIVE SYSTEM SCHEMATIC FOR ONE SECTION OF THE MACHINE, SHOWING HOW THE SIGNALS FOR THE PHASING SYSTEM ARE DERIVED.

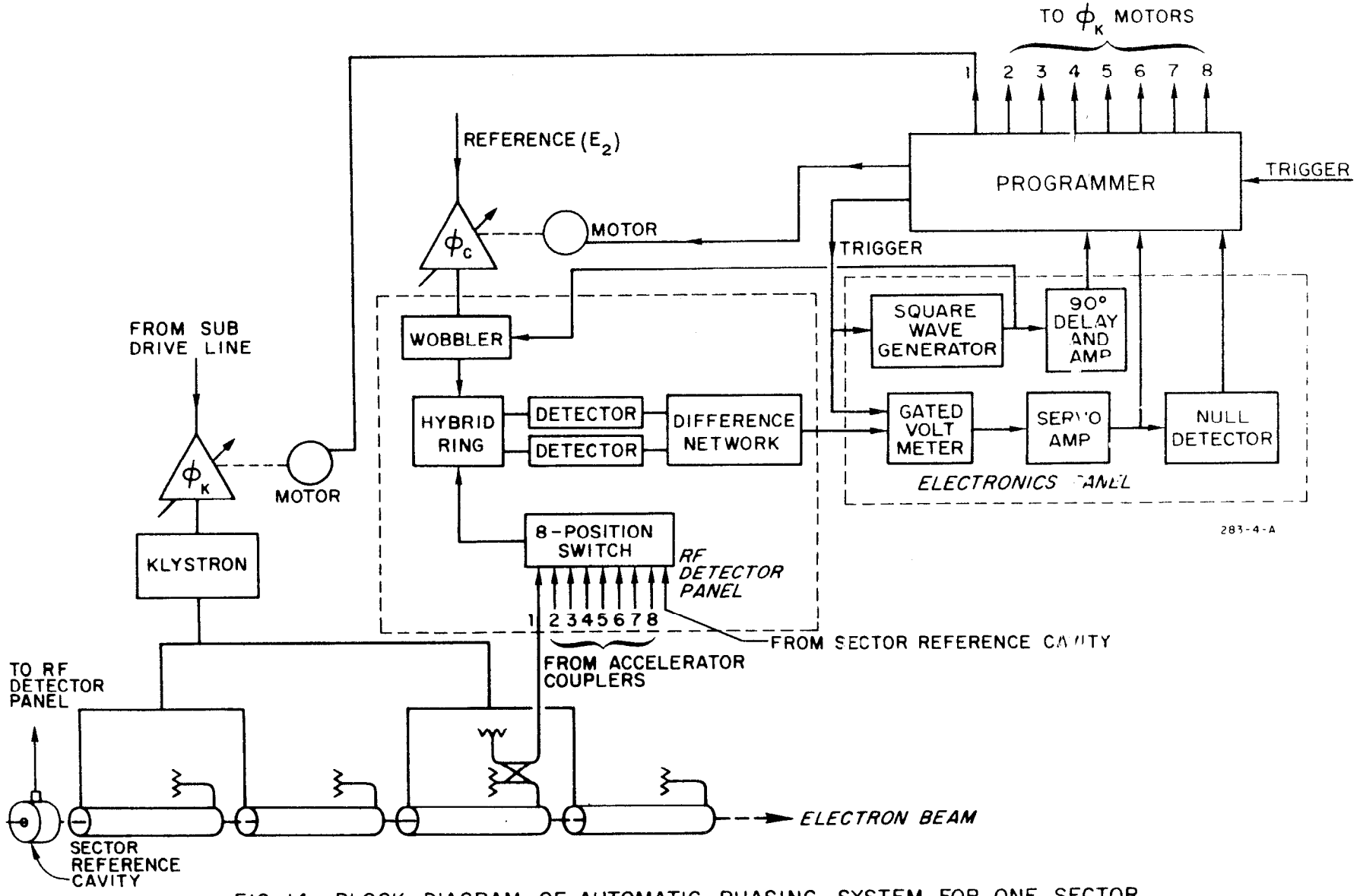

FIG. 14 - BLOCK DIAGRAM OF AUTOMATIC PHASING SYSTEM FOR ONE SECTOR.

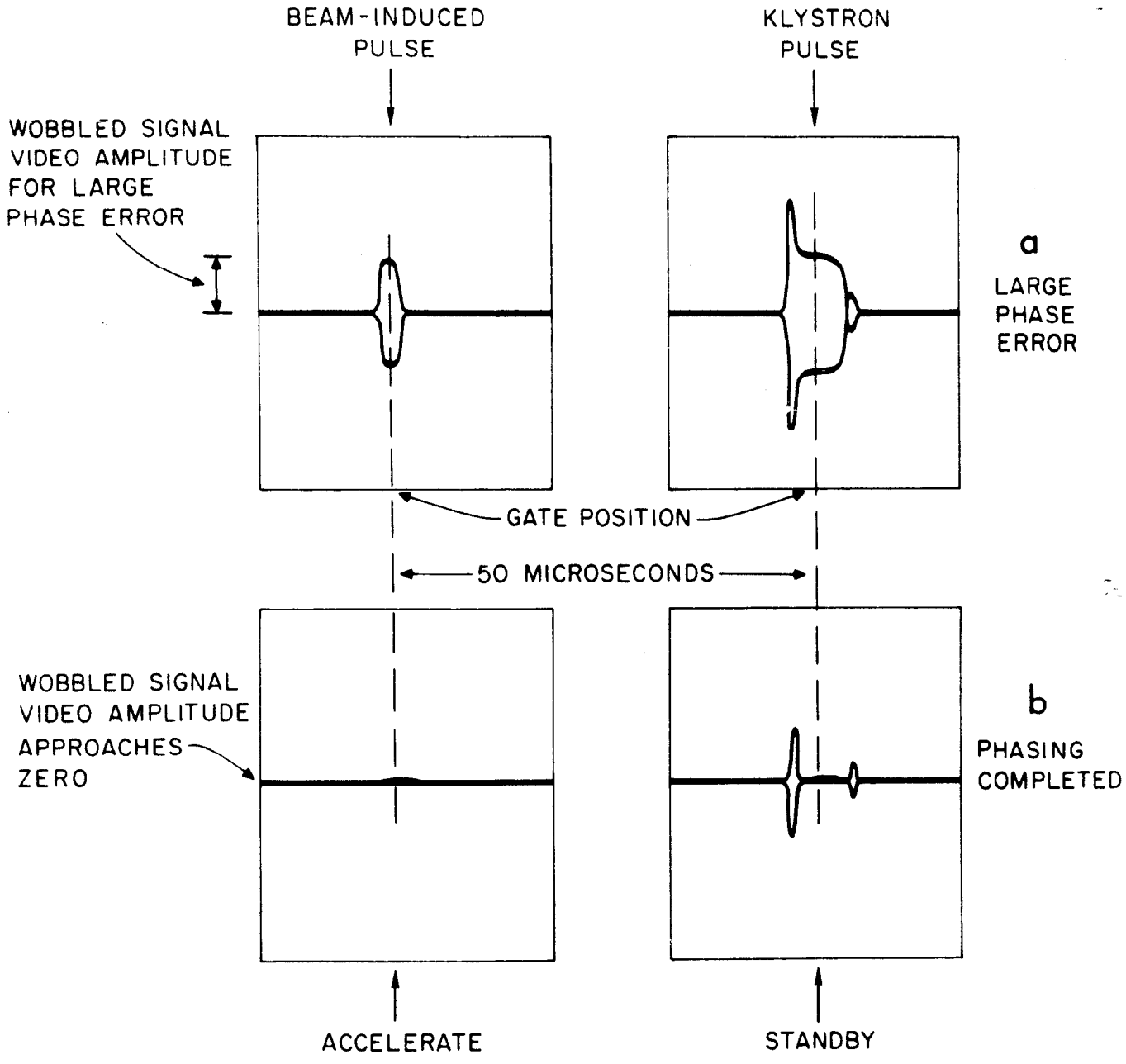

Fig.15--TYPICAL CRO TRACE OF THE VIDEO SIGNAL AT THE OUTPUT OF THE DIODE NETWORK

283-21-A

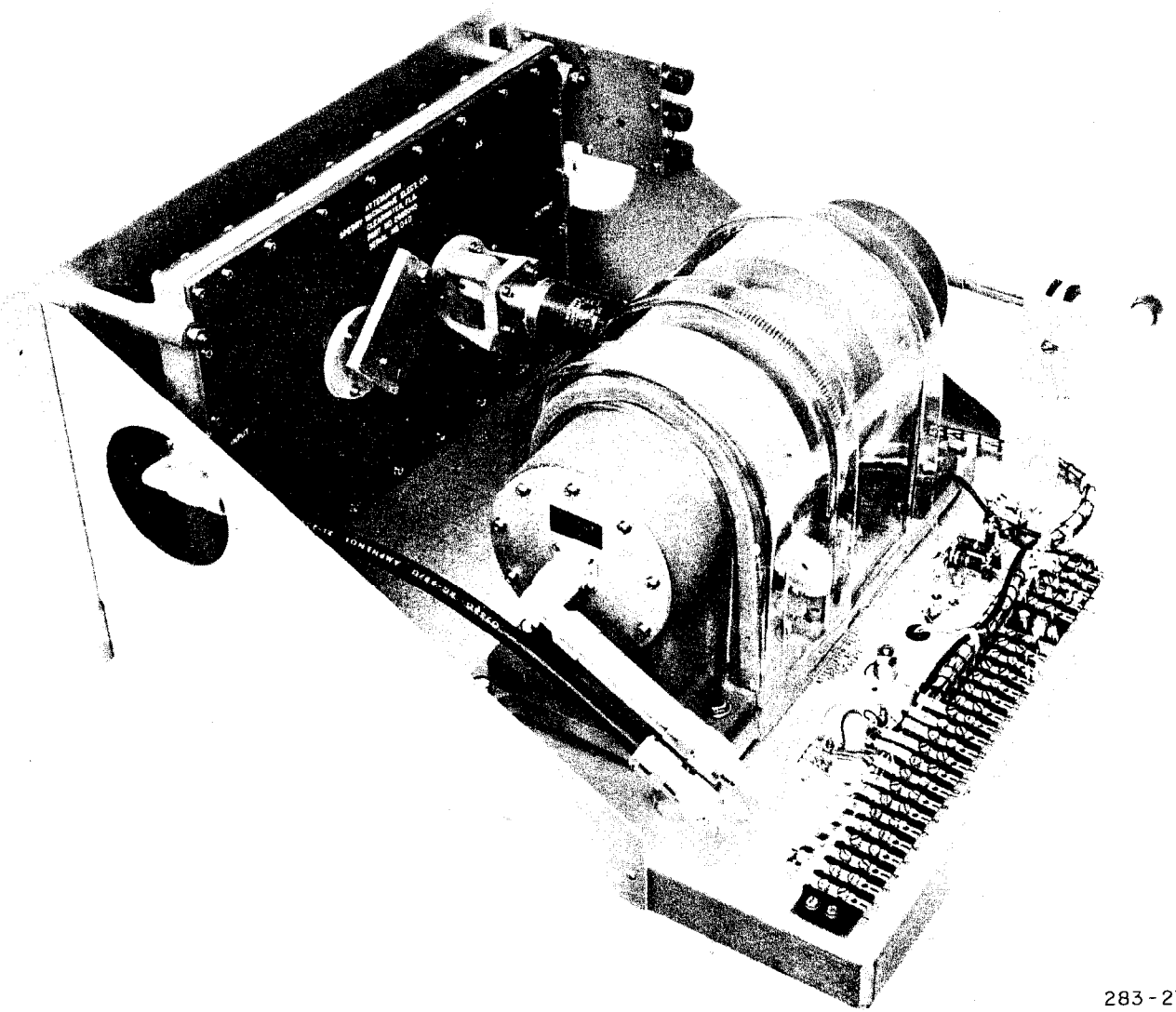

283-27-A

Fig. 16--AN ISOLATOR, PHASE SHIFTER, ATTENUATOR UNIT

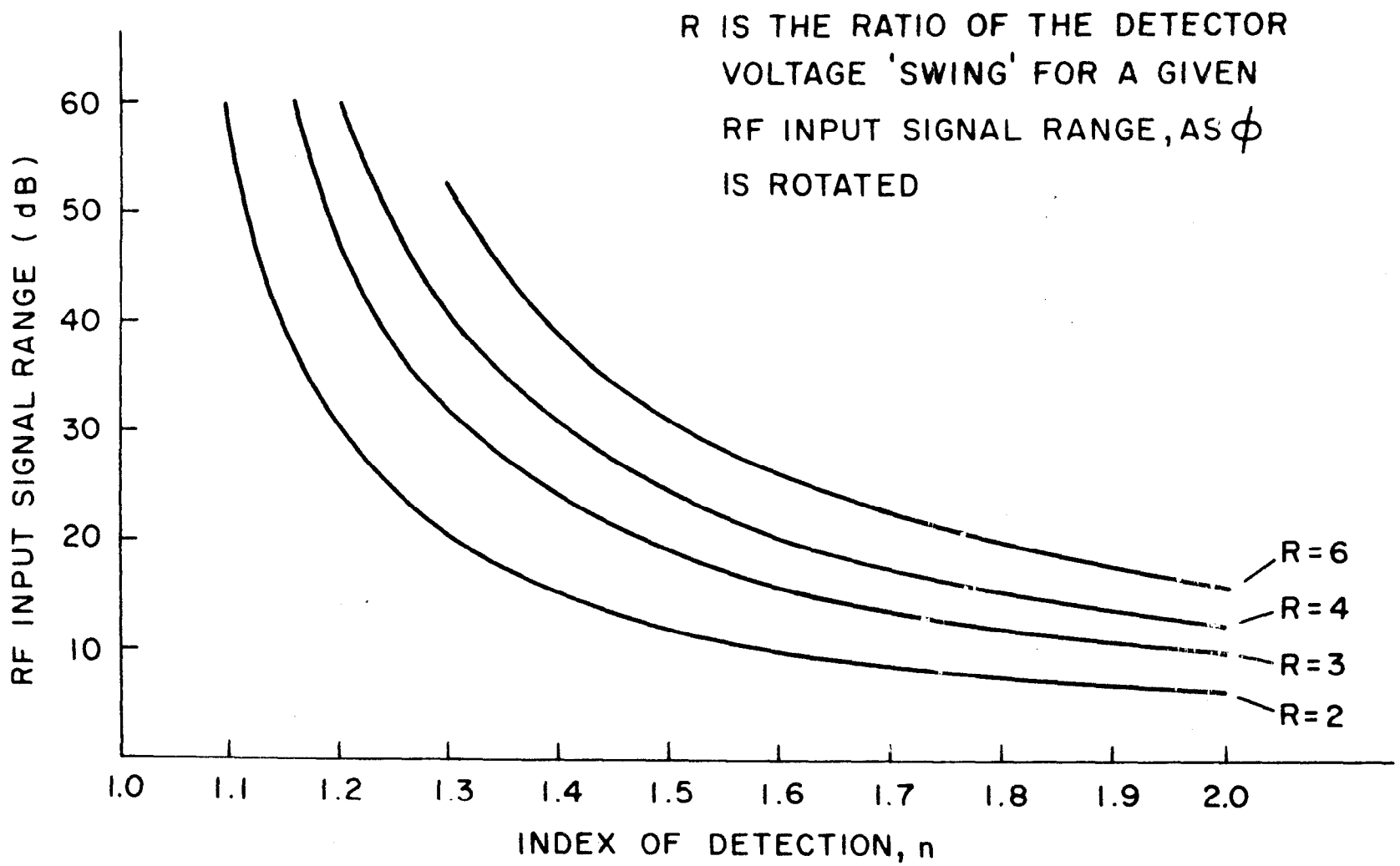

Fig. 17--ILLUSTRATING THE EFFECT OF INCREASING THE DIODE INDEX OF DETECTION

283-23-A

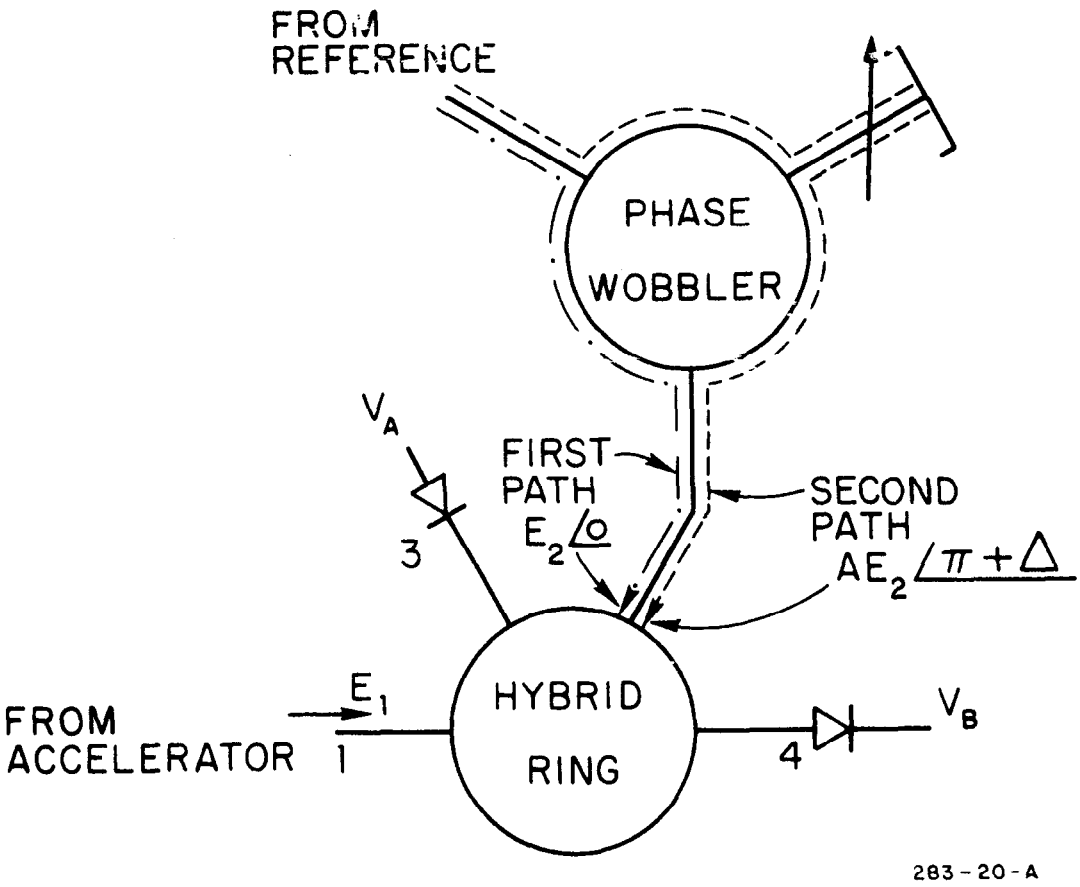

FIG. 18 - ILLUSTRATING THE EFFECT OF AN IMPERFECT WOBBLER.

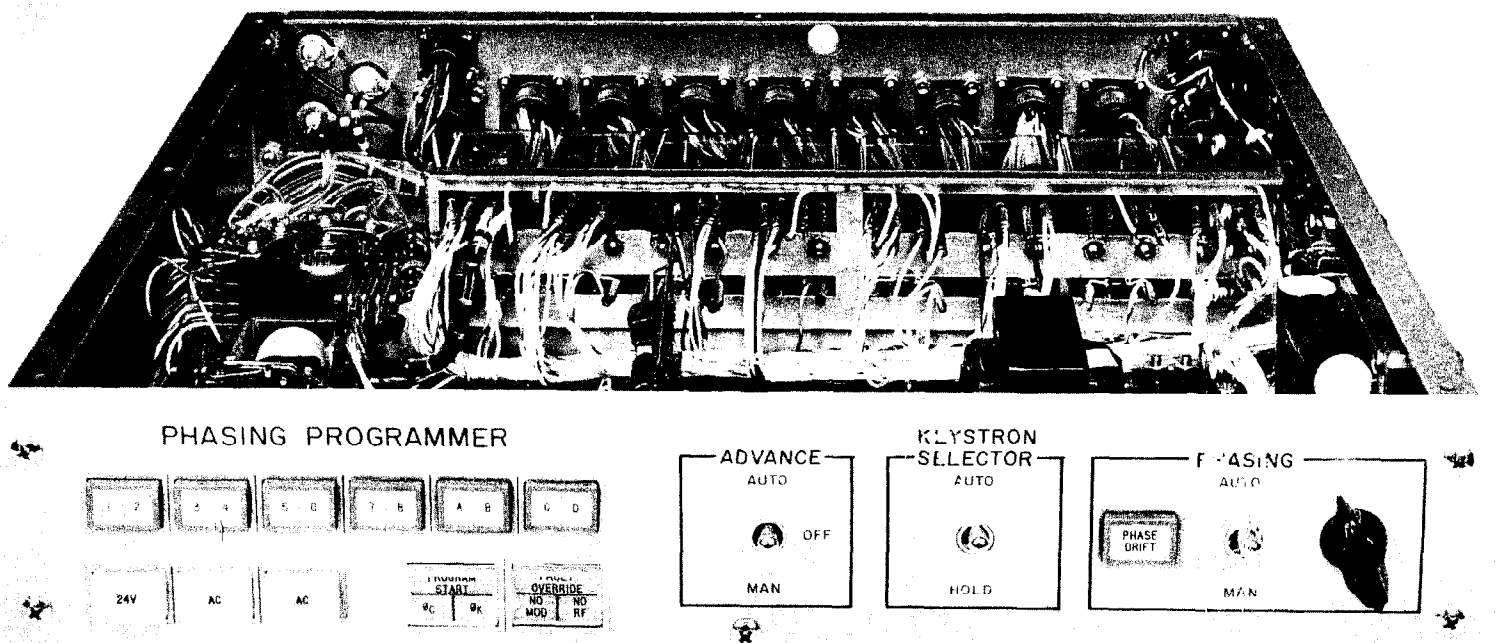

283-28-A

FIG. 19 -- PHASING PROGRAMMER